An irresolute linker: separation, structural and spectroscopic characterization of the two linkage isomers of a Ru(II)-(2-(2′-pyridyl)pyrimidine-4-carboxylic acid) complex.

E. Iengo,[a] N. Demitri,[b] G. Balducci[a] and E. Alessio[a]*

[a] Dipartimento di Scienze Chimiche e Farmaceutiche, Università di Trieste, Via L. Giorgieri 1, 34127 Trieste, Italy. E-mail: alessi@units.it.

[b] Elettra – Sincrotrone Trieste, S.S. 14 Km 163.5 in Area Science Park, 34149 Basovizza – Trieste, Italy.

Electronic Supplementary Information (ESI)

Instrumental Methods. Mono- (^{1}H (500 MHz), ^{13}C (126 MHz), ^{31}P (202 MHz)) and bi-dimensional (^{1}H-^{1}H COSY, ^{1}H-^{13}C HSQC) NMR spectra were recorded on a Varian 500 spectrometer at room temperature. ^{1}H chemical shifts in D_2O were referenced to the internal standard 2,2-dimethyl-2,2-silapentane-5-sulfonate (DSS) at δ = 0.00, while in other solvents were referenced to the peak of residual non-deuterated solvent (δ = 4.33 for CD_3NO_2, 2.50 for DMSO-d_6); ^{31}P chemical shifts were referenced to an external 85% H_3PO_4 standard at 0.00 ppm. Positive ion electrospray mass spectrometry ESI(+) was performed on a Bruker Esquire2000 Mass Spectrometer . Elemental analysis was performed at the Department of Chemistry of the University of Bologna (Italy). For the ^{1}H NMR titration, pH values in D_2O were measured at 298 K directly in the NMR tube using an AMEL (model 334B) pH meter equipped with an Ingold micro electrode. The pH values were adjusted with diluted $DClO_4$ and NaOD solutions. No correction was applied for the effect of deuterium on the glass electrode.

Experimental Procedures.

The linker cppH·HNO_3 was prepared as described in ref. 6. An improved synthetic procedure, with respect to that reported in ref. 10, was adopted for the preparation of the precursor complex [Ru([9]aneS_3)Cl_2(PTA)] (**1**), using CH_3CN instead of CH_3NO_2 as solvent.

[Ru([9]aneS_3)(bpy)(PTA)][Cl]$_2$ (3). A 70 mg amount of [Ru([9]aneS_3)Cl_2(PTA)] (**1**, 0.137 mmol) was partially dissolved in 10 mL of methanol. A slight excess of bpy (32 mg, 0.204 mmol, bpy/Ru = 1.5) was added and the mixture was heated to reflux until no residual undissolved precursor remains (at least 12h). After cooling, the final deep-yellow solution was filtered over celite (to remove traces of unreacted **1**) and concentrated to *ca.* 2 mL. Diethyl ether was slowly added dropwise until saturation. Yellow crystals of the product formed within 24 \h and were filtered, washed with diethyl ether and vacuum dried. Yield: 70.7 mg (77%). Complex **3** is well soluble in H_2O, EtOH and MeOH, partially soluble in CH_3NO_2 and CH_3CN, insoluble in acetone, CH_2Cl_2 and $CHCl_3$. M_W = 665.66; $C_{22}H_{32}N_5Cl_2PRuS_3$, requires: C, 39.69; H, 4.84; N, 10,52; S, 14.45%. Found: C, 39.50; H, 4.76; N, 10.64; S, 14.18%. ^{1}H-NMR (D_2O, see Figure S2), δ (ppm): 8.87 (d, 2H, H6 + H6′), 8.60 (d, 2H, H3 + H3′), 8.28 (t, 2H, H4 + H4′), 7.73 (t, 2H, H5 + H5′), 4.37 (ABq, 6H, $\Delta\delta_{AB}$ = 0.09, J_{AB} = 13.0 Hz, NCH_2N PTA), 3.79 (s, 6H, NCH_2P PTA), 3.2 – 2.5 (m, 12H, [9]aneS_3). ^{13}C-NMR (from the HSQC spectrum, D_2O), δ (ppm): 153.0 (C6 + C6′), 139.7 (C4 + C4′), 128.3 (C5 + C5′), 125.0 (C3 + C3′), 70.4 (NCH_2N PTA), 48.1 (NCH_2P PTA), 36.8, 33.0, 29.7 (CH_2 [9]aneS_3). ^{31}P-NMR (D_2O), δ (ppm): –36.78 (s, PTA).

[Ru([9]aneS_3)(bpy)(PTA)][PF_6]$_2$ (3PF_6). The first part of the procedure was the same as for **3**. Anion metathesis was performed as follows: to the final deep yellow solution an excess of NH_4PF_6

(67.5 mg, 0.414 mmol, NH_4PF_6/Ru = 3) dissolved in 3 mL of methanol was added dropwise, inducing the immediate precipitation of the product as a yellow solid that was filtered, washed with methanol, diethyl ether and vacuum dried. Yield: 80.8 mg (67%). Complex **3PF$_6$** is well soluble in CH_3NO_2 and CH_3CN, partially soluble in acetone, poorly soluble in H_2O, MeOH, and $CHCl_3$. Crystals suitable for X-ray diffraction were obtained by dissolving the crude product in acetonitrile (70 mg in ca. 3 mL) followed by slow dropwise addition of diethyl ether until saturation (yield 62 mg). M_W = 884.67; $C_{22}H_{32}N_5F_{12}P_3RuS_3 \cdot CH_3CN$ requires: C, 31.14; H, 3.81; N, 9.07; S, 10.38%. Found: C, 31.35; H, 3.92; N, 8.94; S, 10.50%. ^{1}H-NMR (CD_3NO_2, see Figure S1), δ (ppm): 8.88 (d, 2H, H6 + H6′), 8.59 (d, 2H, H3 + H3′), 8.30 (t, 2H, H4 + H4′), 7.74 (t, 2H, H5 + H5′), 4.33 (ABq, 6H, $\Delta\delta_{AB}$ = 0.09, J_{AB} = 13.8 Hz, NC*H*$_2$N PTA), 3.84 (s, 6H, NCH$_2$P PTA), 3.3 – 2.6 (m, 12H, [9]aneS$_3$). ^{13}C-NMR (from the HSQC spectrum, CD_3NO_2), δ (ppm): 153.1 (C6 + C6′), 139.6 (C4 + C4′), 128.4 (C5 + C5′), 124.8 (C3 + C3′), 71.9 (N*C*H$_2$N PTA), 49.5 (N*C*H$_2$P PTA), 36.9, 33.1, 29.8 ([9]aneS$_3$). ^{31}P-NMR (CD_3NO_2), δ (ppm): –44.55 (s, PTA).

[Ru([9]aneS$_3$)(cppH)(PTA)][Cl]$_2$ (2). An 80 mg amount of [Ru([9]aneS$_3$)Cl$_2$(PTA)] (**1**) (0.157 mmol) was dissolved in 10 mL of H_2O. A slight excess of cppH·HNO_3 (62 mg, 0.235 mmol, cppH/Ru = 1.5) was added and the yellow solution was heated to reflux for 5h, turning orange-yellow (to be noted that no reaction occurred in refluxing ethanol or methanol, even for prolonged reaction times, most likely because of the low solubility of both species in such solvents). Evaporation of the solvent under reduced pressure afforded a sticky orange-red solid that was sonicated at length with 20 mL of acetone (where it is insoluble) until an amorphous yellow solid was obtained. It was filtered, washed with acetone and diethyl ether and vacuum dried. Yield 90 mg (81%). The complex is well soluble in H_2O, EtOH, MeOH and DMSO. Crude **2** was recrystallized by layering acetone on top of a concentrated aqueous solution (pH = ca. 2, depending on the batch), affording pure **2** as a mixture of crystals of ***2N^p*** and ***2N^o*** (total yield 80%) that were characterized by elemental analysis, mass spectrometry, and 1D and 2D NMR spectroscopy both as a mixture and after they were separated manually under the microscope.

Compound **2**: M_W = 710.65, $C_{22}H_{31}N_6Cl_2O_2PRuS_3$, requires: C, 37.18; H, 4.39; N, 11,82; S, 13.53%. Found: C, 37.30; H, 4.48; N, 11.69; S, 13.42%.

2N^p: ^{1}H-NMR (D_2O) δ ppm: 9.13 (d, 1H, H6, ^3J = 4.90 Hz), 8.91(d, 1H, H6', ^3J = 8.0 Hz), 8.85 (d, 1H, H3', ^3J = 5.5 Hz), 8.34 (t, 1H, H5', ^3J = 7.80), 7.87 (t, 1H, H4', ^3J = 7.20), 7.64 (d, 1H, H5, ^3J = 4.90 Hz), 4.70 (ABq 6H, $\Delta\delta_{AB}$ = 0.03, J_{AB} = 12.8 Hz, NC*H*$_2$N PTA), 4.16 (br s, 6H, NC*H*$_2$P PTA), 3.40 (m, 2H), 3.34 (m, 2H), 3.21 (m, 2H), 2.98 (m, 1H), 2.85 (m, 1H), 2.75 (m, 1H), 2.67 (m, 1H), 2.56 (m, 1H), 2.37 (m, 1H). ^{13}C-NMR (D_2O), δ (ppm): 162.18 (C6), 154.96 (C3'), 142.78 (C5'), 132.96 (C4'), 130.98 (C6'), 121.78 (C5), 70.76+70.71 (N*C*H$_2$N PTA), 47.21+47.10 (N*C*H$_2$P PTA),

39.07-27.34 ([9]aneS$_3$). ^{31}P-NMR (D_2O), δ ppm: –30.18 (PTA). ES mass spectrum (*m*/*z*) (positive mode): 595 $(M - H - CO_2)^+$.

2*N*^{o}: ^{1}H-NMR (D_2O) δ ppm: 9.28 (d, 1H, H6, ^3J = 5.80), 9.04(d, 1H, H6', ^3J = 7.90), 8.88 (d, 1H, H3', ^3J = 5.50), 8.39 (t, 1H, H5', ^3J = 7.80), 8.16 (d, 1H, H5, ^3J = 5.80), 7.89 (t, 1H, H4', ^3J = 7.0), 4.70 (ABq 6H, $\Delta\delta_{AB}$ = 0.03, J_{AB} = 12.7 Hz, NC*H*$_2$N PTA), 4.01 (br s, 6H, NC*H*$_2$P PTA), 3.40 (m, 1H), 3.28 (m, 2H), 3.13 (m, 2H), 3.01 (m, 4H), 2.71 (m, 4H). ^{13}C-NMR (D_2O), δ (ppm):): 161.74 (C6), 153.46 (C3'), 140.59 (C5'), 130.57 (C4'), 128.33 (C6'), 122.40 (C5), 70.68+70.58 (N*C*H$_2$N PTA), 47.05+46.80 (N*C*H$_2$P PTA), 37.35-29.00 ([9]aneS$_3$). ^{31}P-NMR (D_2O), δ ppm: –30.96 (s, PTA). ES mass spectrum (*m*/*z*) (positive mode): 639 ([Ru^{II}([9]aneS$_3$)(cpp)(PTA)]$^+$, $(M - H)^+$), 595 $(M^+ - H - CO_2)^+$).

[Ru([9]aneS$_3$)(mpp)(PTA)][Cl$_2$] (**4**)**.** An 80 mg amount of [Ru([9]aneS$_3$)Cl$_2$(PTA)] (**1**) (0.157 mmol) was partially dissolved in 15 mL of MeOH. A slight excess of mpp (40.2 mg, 0.23 mmol, mpp/Ru = 1.5), which is well soluble in MeOH, was added and the mixture was heated to reflux for 9h, i.e. until the solid starting complex disappeared completely, yielding a clear deep-yellow solution. Evaporation of the solvent under reduced pressure afforded a deep-yellow oil that was sonicated at length with 20 mL of acetone (where it is insoluble) until an amorphous yellow solid was obtained. It was filtered, washed with acetone and diethyl ether and vacuum dried. Yield 100 mg (93%). The complex is well soluble in H_2O, EtOH, MeOH and DMSO and completely insoluble in $CHCl_3$. It was characterized by elemental analysis, mass spectrometry, and 1D and 2D NMR spectroscopy. Compound **4**: M_W = 680.70, $C_{22}H_{33}N_6Cl_2PRuS_3$, requires: C, 38.82; H, 4.88; N, 12,34; S, 14.13%. Found: C, 38.70; H, 4.78; N, 12.23; S, 14.28%. In the ^{1}H and ^{13}C NMR spectra, only the resonances of the major isomer **4*N*^{p}** are reported. In the proton spectrum, most of the resonances of the minor isomer **4*N*^{o}** are overlapped with those of **4*N*^{p}**. Only in the ^{31}P NMR spectrum the singlets of both isomers are clearly distinguishable. ^{1}H-NMR **4*N*^{p}** (D_2O), δ (ppm): 8.90 (d, 1H, H6', ^3J = 5.90), 8.89 (d, 1H, H6, ^3J = 5.0), 8.87 (d, 1H, H3', ^3J = 4.5), 8.33 (t, 1H, H4', ^3J = 7.80), 7.83 (t, 1H, H5', ^3J = 7.09), 7.65 (d, 1H, H5, ^3J = 6.0), 4.37 (ABq 6H, $\Delta\delta_{AB}$ = 0.03, J_{AB} = 13.14 Hz, NC*H*$_2$N PTA), 3.80 (br s, 6H, NC*H*$_2$P PTA), 3.21 (m, 2H), 3.07 (m, 2H), 2.95 (m, 4H), 2.79 (s, 3H, -CH$_3$), 2.66 (m, 4H). ^{13}C-NMR **4*N*^{p}** (from the HSQC spectrum, D_2O), δ (ppm): 158.70 (C6'), 153.31 (C3'), 139.96 (C4'), 129.97 (C5'), 127.38 (C6), 123.54 (C5), 70.25+70.16 (N*C*H$_2$N PTA), 47.95 (N*C*H$_2$P PTA), 36.96-29.53 ([9]aneS$_3$). 23.47 (-CH$_3$). ^{31}P-NMR (D_2O), δ (ppm): –39.42 (s, PTA **4*N*^{p}**); –39.98 (s, PTA **4*N*^{o}**). ES mass spectrum (*m*/*z*) (positive mode): 645 $(M + Cl)^+$, 609 $(M - H)^+$.

Crude **4** was recrystallized by layering acetone on top of a concentrated aqueous solution (pH 8.10) affording pure crystals of **4*N*^{p}** suitable for X-ray investigation (Yield 80%).

^{1}H NMR pH titration of cppH in D_2O.

The ^{1}H NMR spectrum of cppH in D_2O depends strongly on pH, as we could verify through an NMR titration. A saturated D_2O solution of cppH·HNO_3 has a pH below 2 and its ^{1}H NMR spectrum is quite different from that reported in ref. 6. Upon increasing the pH, the resonances of all six protons are shifted upfield: the chemical shifts of the resonances of the two protons on the pyrimidine ring (H5 and H6) change most between pH 2 and 4.8 and remain basically unchanged for higher pH, whereas the chemical shifts of the resonances of the four protons on the pyridine ring change most between pH 2.5 and 6, and remain basically unchanged for pH > 6. These results are consistent with the following considerations: *i*) at pH < 2 both the pyridine N atom (N1') and the less basic pyrimidine N1 atom (i.e. N^p) are protonated; consistent with the protonation of N^p the resonances of both H5 and H6 are dd's for pH ≤ 2.5, whereas they become simple doublets at pH ≥ 3.9. *ii*) Upon increasing the pH, deprotonation of the pyrimidine N atom occurs first (estimated pK_a for N1 (i.e. N^p) = ca. 3.0), followed by deprotonation of the pyridine N atom (estimated pK_a for N1' = ca. 4.7).

To be noted that the two unresolved dd's belonging to H3' and H6' **invert their relative positions** upon varying the pH, thus their correct attribution is questionable. We argue that at low pH, where the pyridine N atom is protonated, the most downfield dd can be reasonably assigned to H6', i.e. to the most deshielded proton adjacent to the NH^+ moiety (consistent with this assignment, the change in chemical shift of this resonance upon deprotonation of N1' is much larger than that of the other unresolved dd, thus safely assigned to H3', i.e. the proton farthest from N1').

The NMR spectrum reported in ref. 6 corresponds to that measured by us for pH > 6, and therefore we notice that the assignments have an inconsistency: the unresolved dd at ca. δ = 8.26 belongs to H3' rather than to H5, whereas the sharp doublet at ca. δ = 7.80 belongs to H5 rather than to H3'. This consideration is relevant for the correct assignments of the resonances of coordinated cppH.

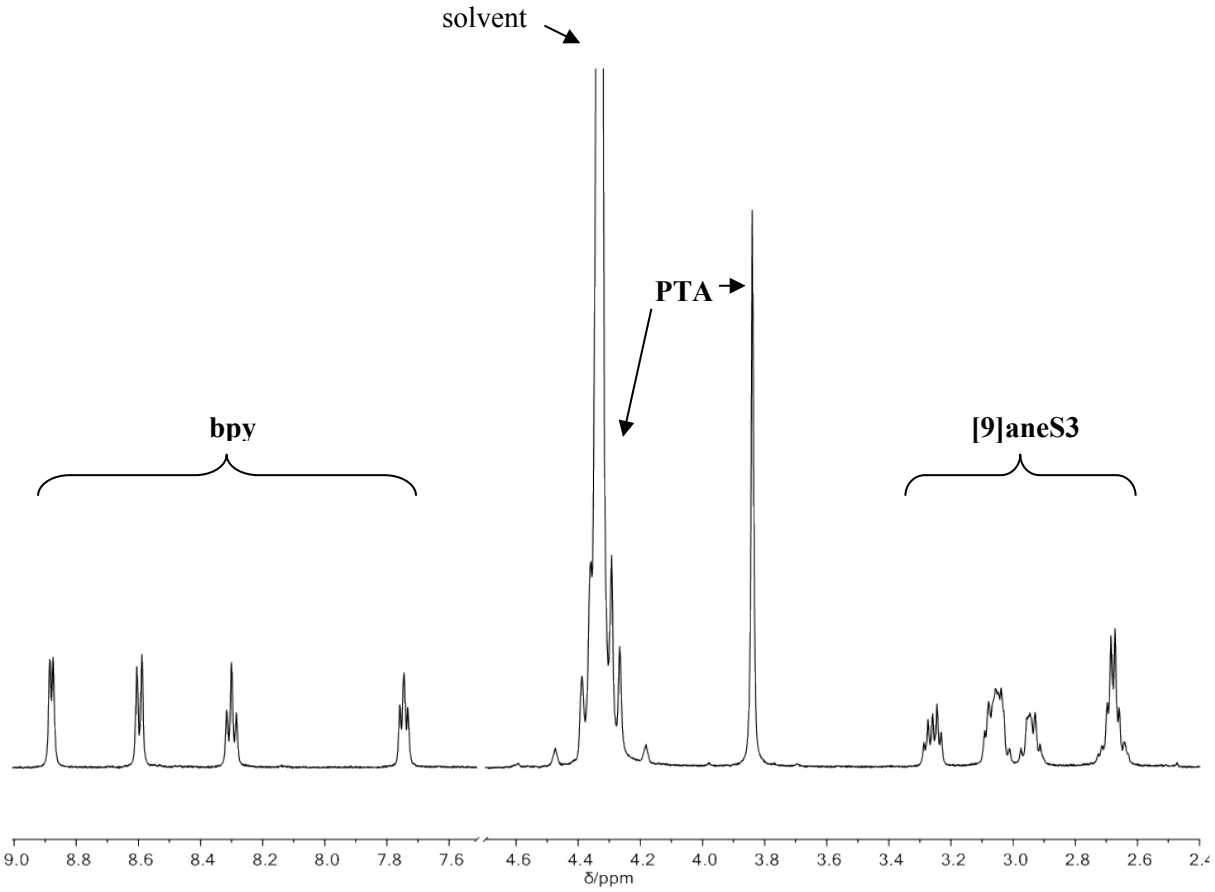

Figure S1. ^{1}H NMR spectrum of [Ru([9]aneS$_3$)(bpy)(PTA)][PF$_6$]$_2$ (**3PF$_6$**) in CD_3NO_2.

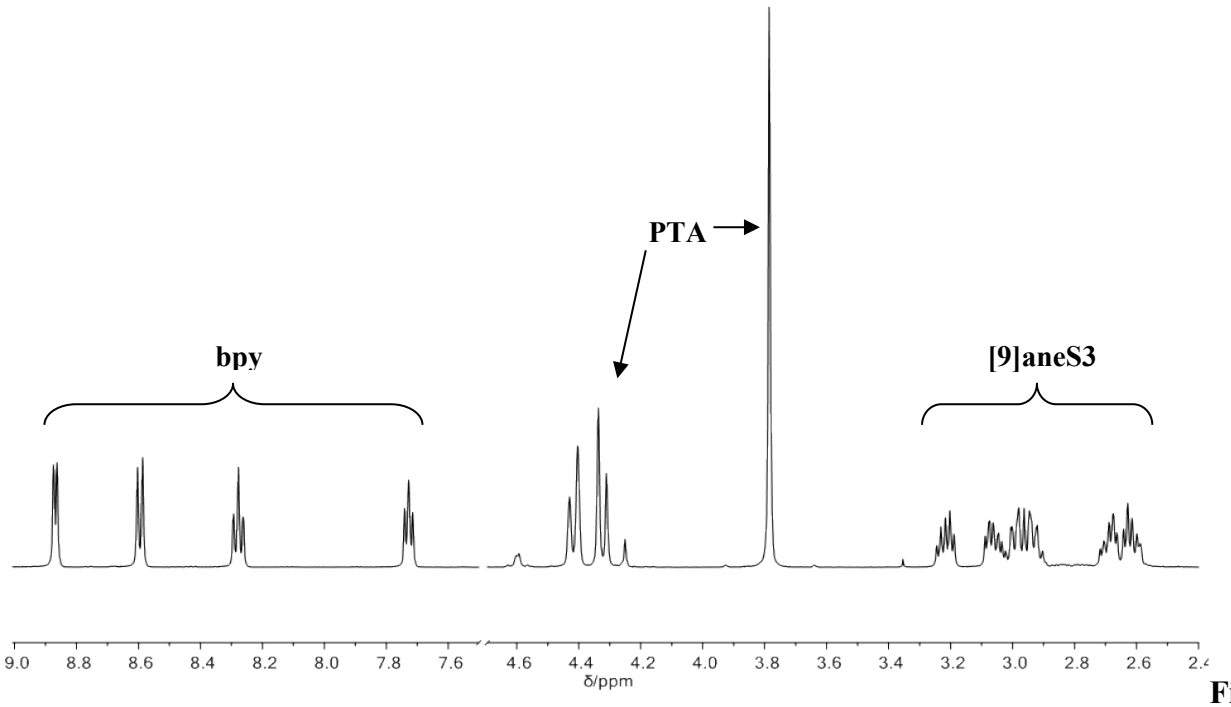

Figure S2. ^{1}H NMR spectrum of [Ru([9]aneS$_3$)(bpy)(PTA)][Cl]$_2$ (**3**) in D_2O.

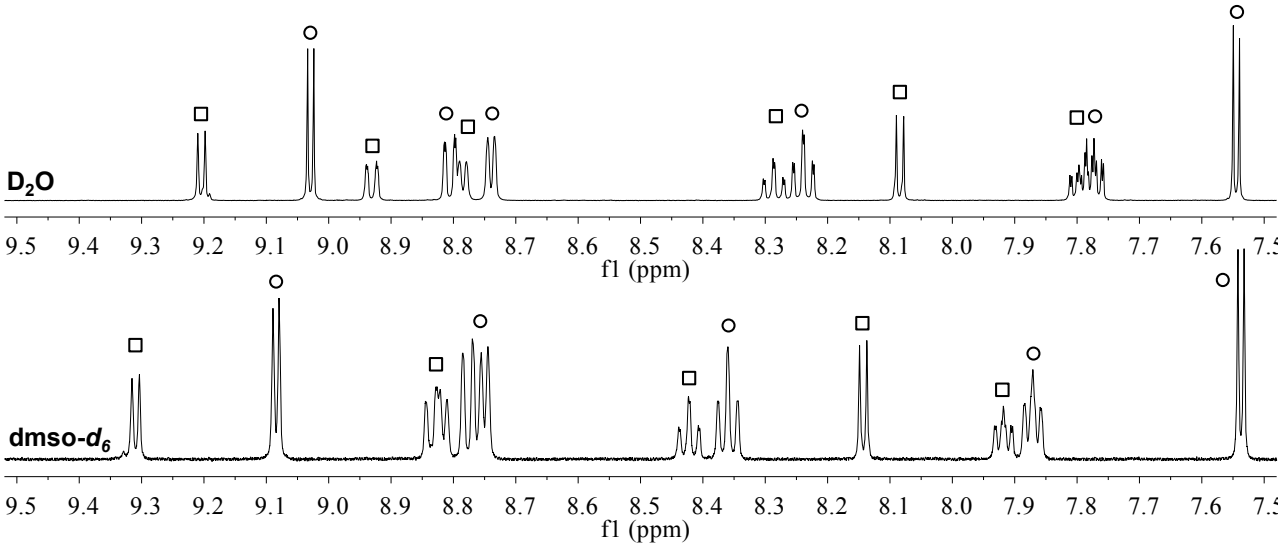

Figure S3. ^{1}H NMR spectrum (cppH region) of crude **2** in D_2O (top) and in dmso-d_6 (bottom).

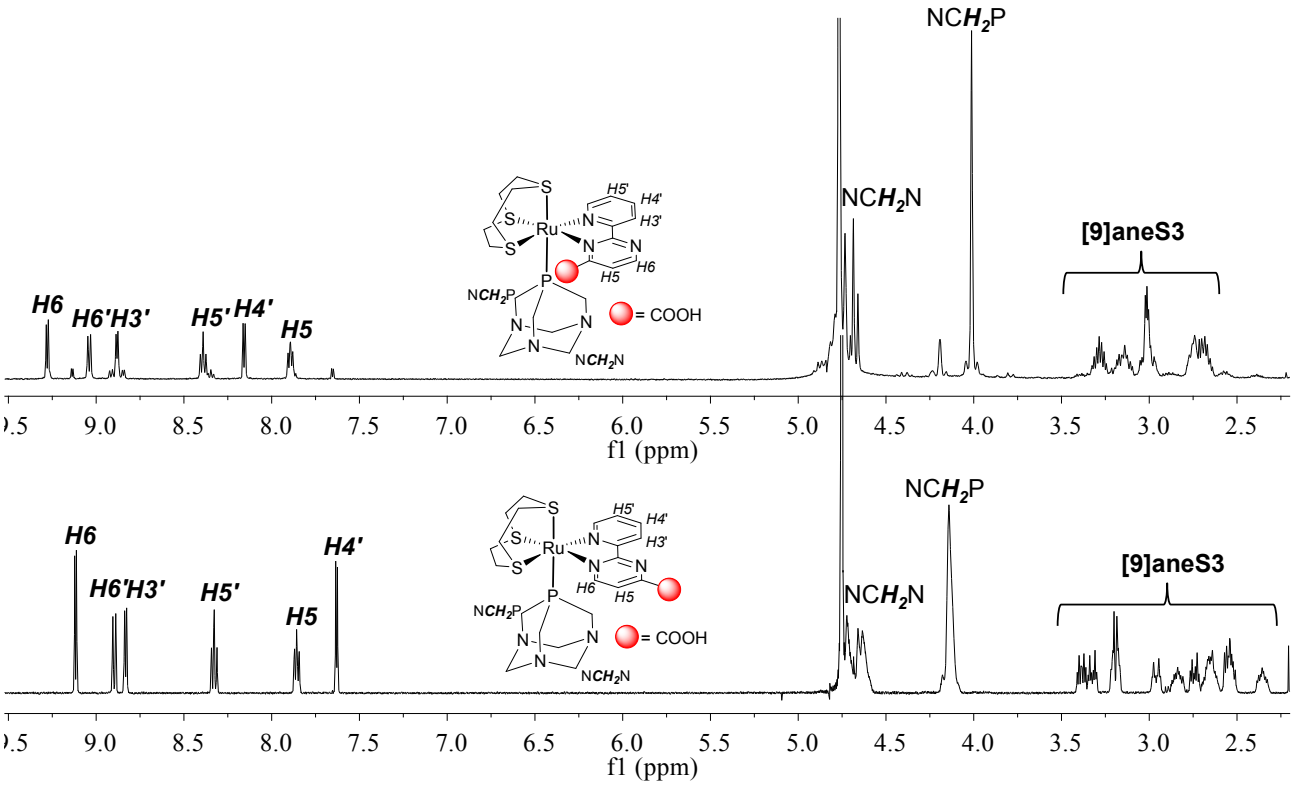

Figure S4. ^{1}H NMR spectrum of **2*N*^{p}** (top) and **2*N*^{o}** (bottom) in D_2O.

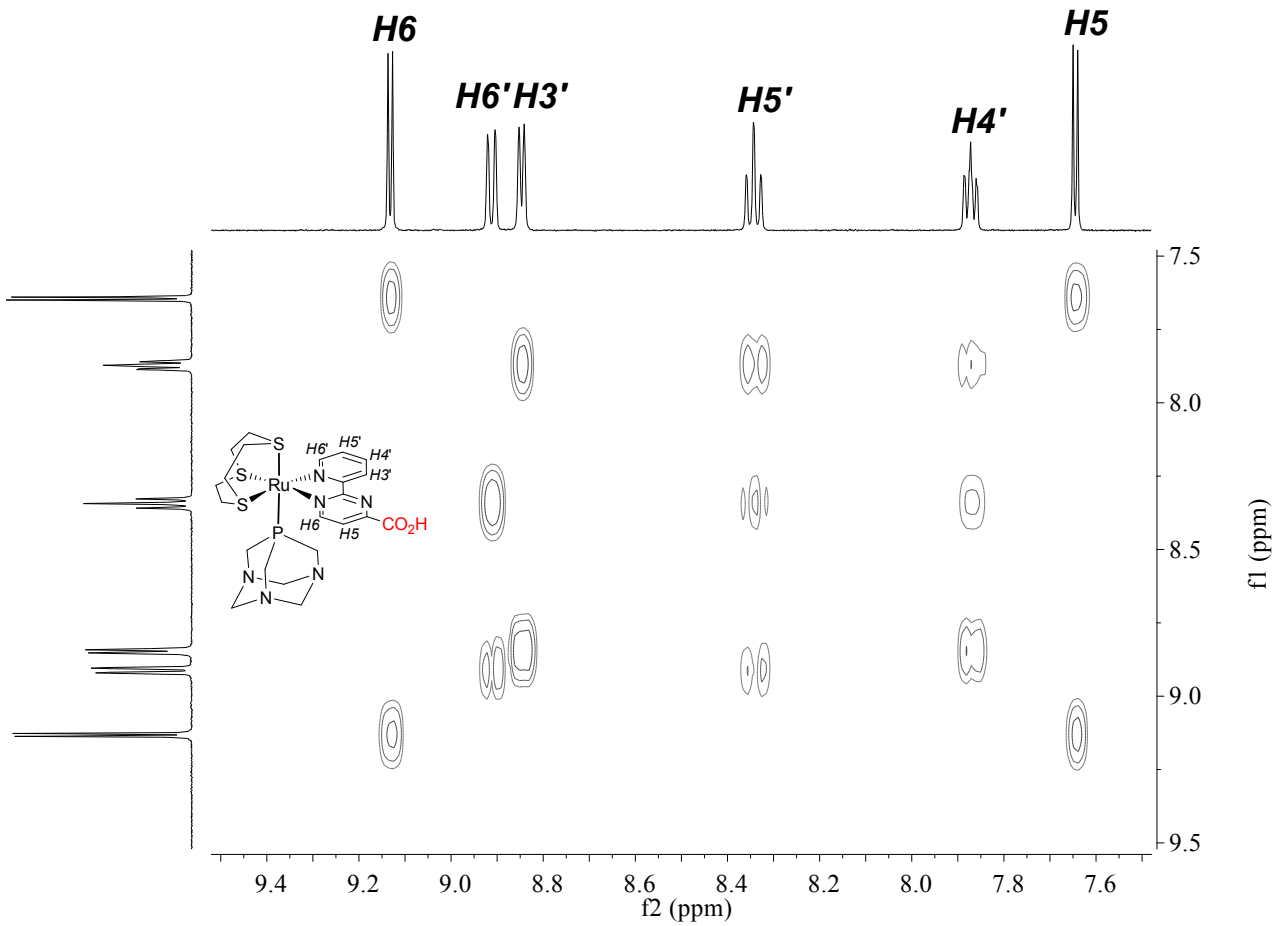

Figure S5. H-H COSY spectrum (cppH region) of **2*N*^{p}** in D_2O, with labeling scheme.

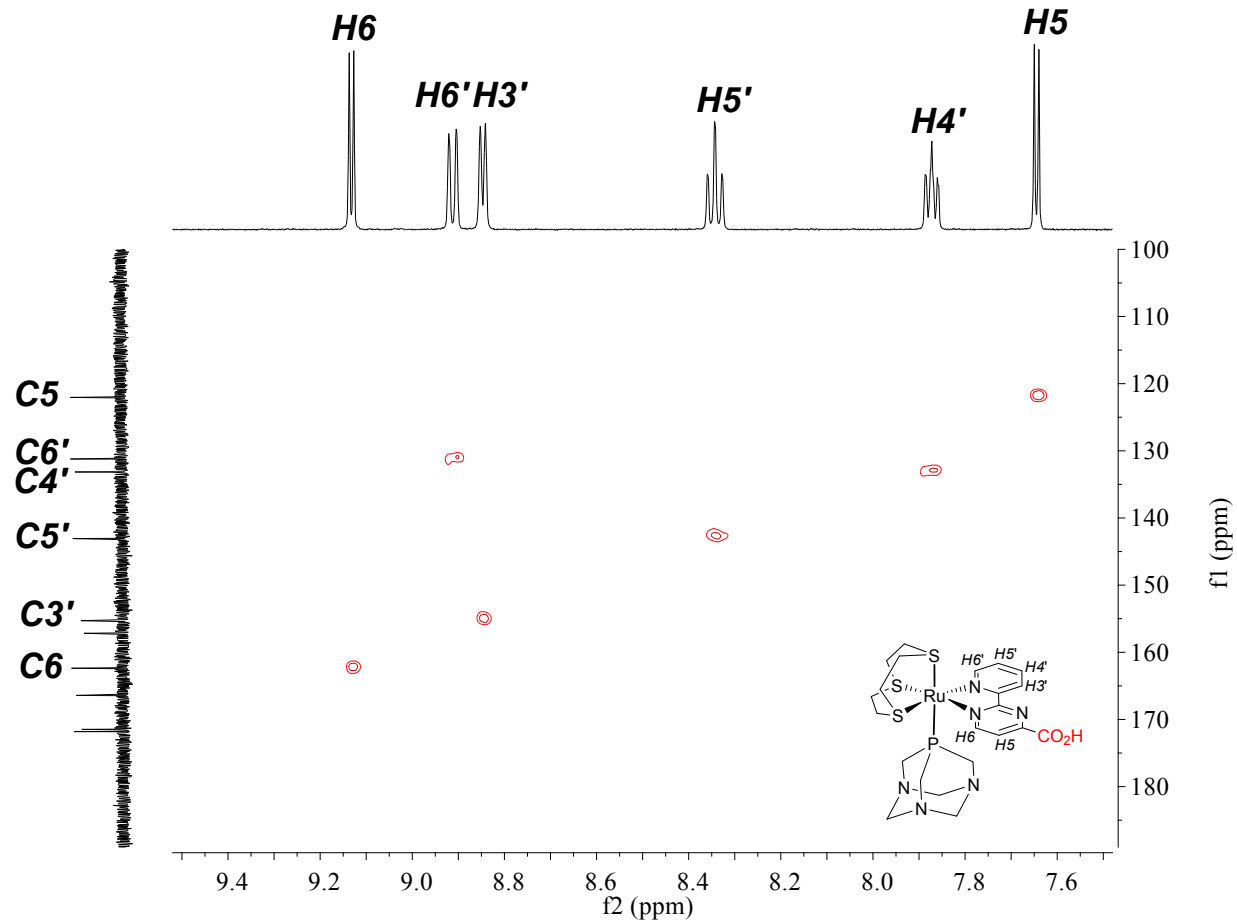

Figure S6. H-C HSQC spectrum (cppH region) of **2*N*^{p}** in D_2O, with labeling scheme.

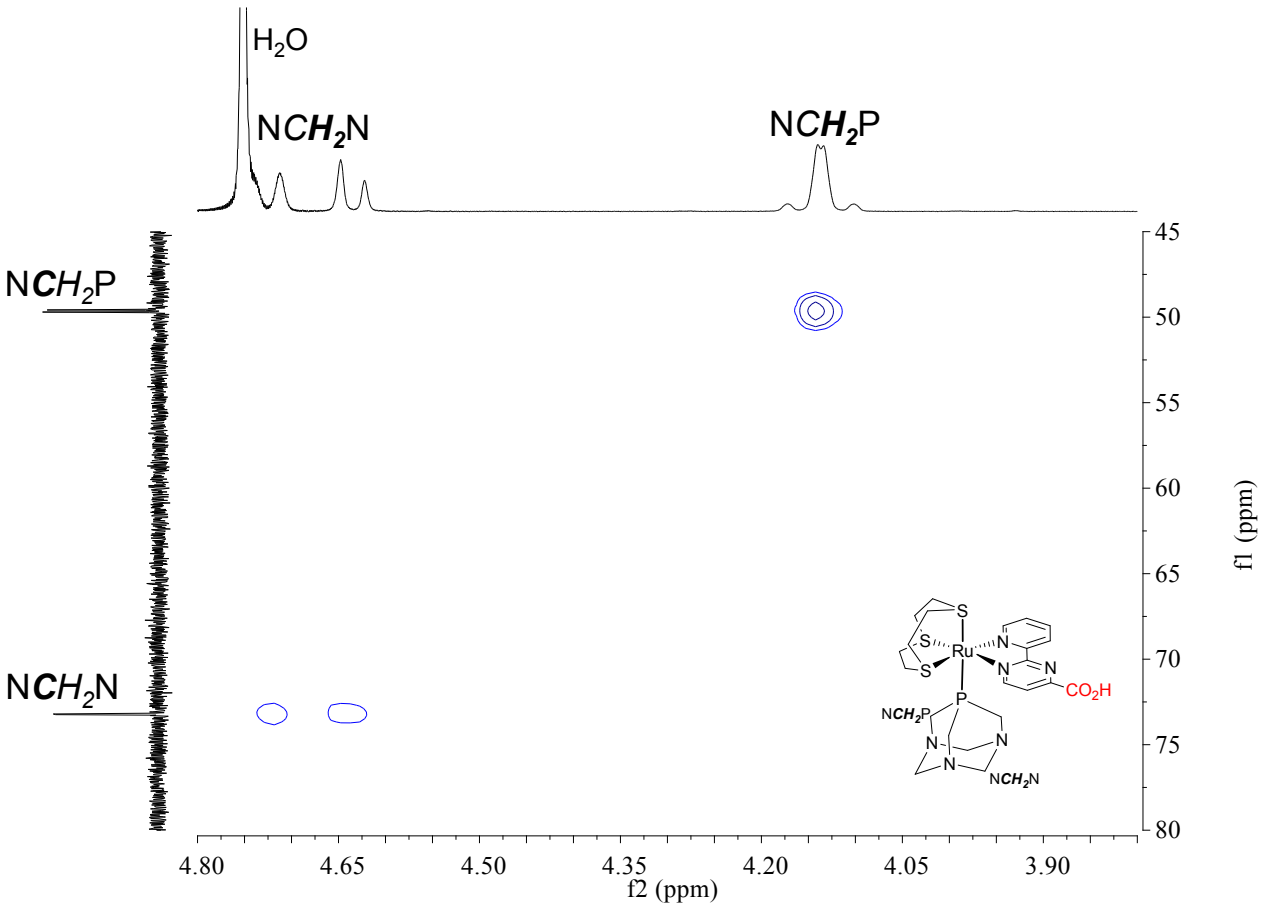

Figure S7. H-C HSQC spectrum (PTA region) of **2*N*^{p}** in D_2O, with labeling scheme.

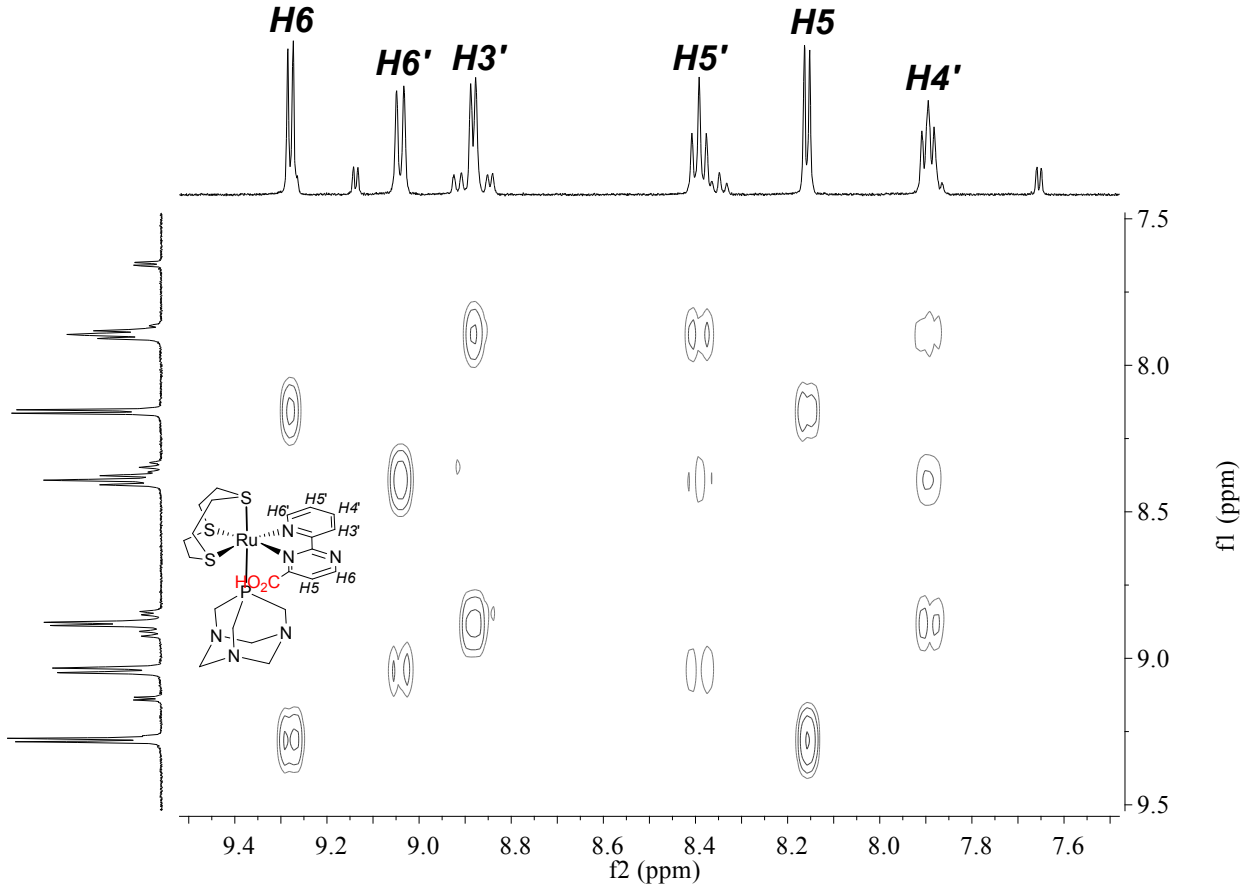

Figure S8. H-H COSY spectrum (cppH region) of **2*N*^{o}** in D_2O, with labeling scheme.

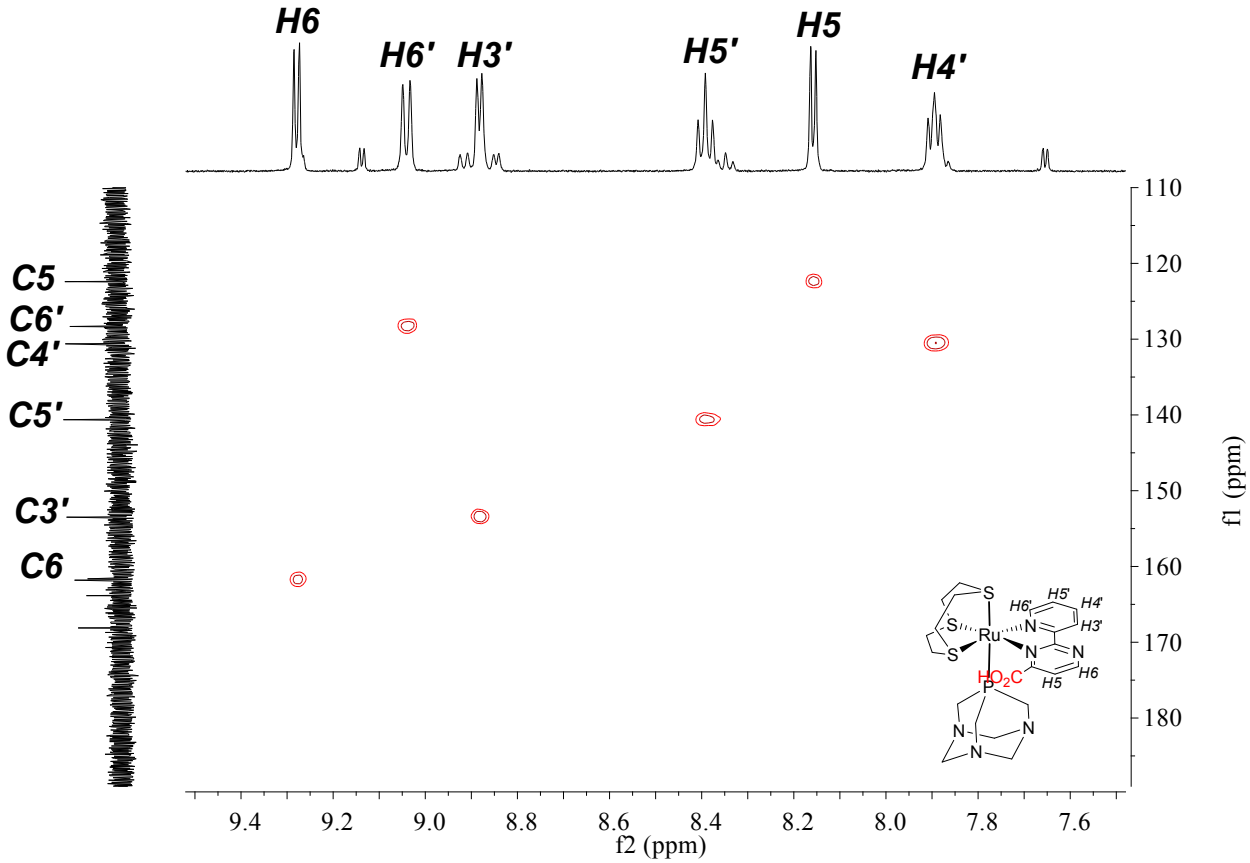

Figure S9. H-C HSQC spectrum (cppH region) of **2*N^o^*** in D_2O, with labeling scheme.

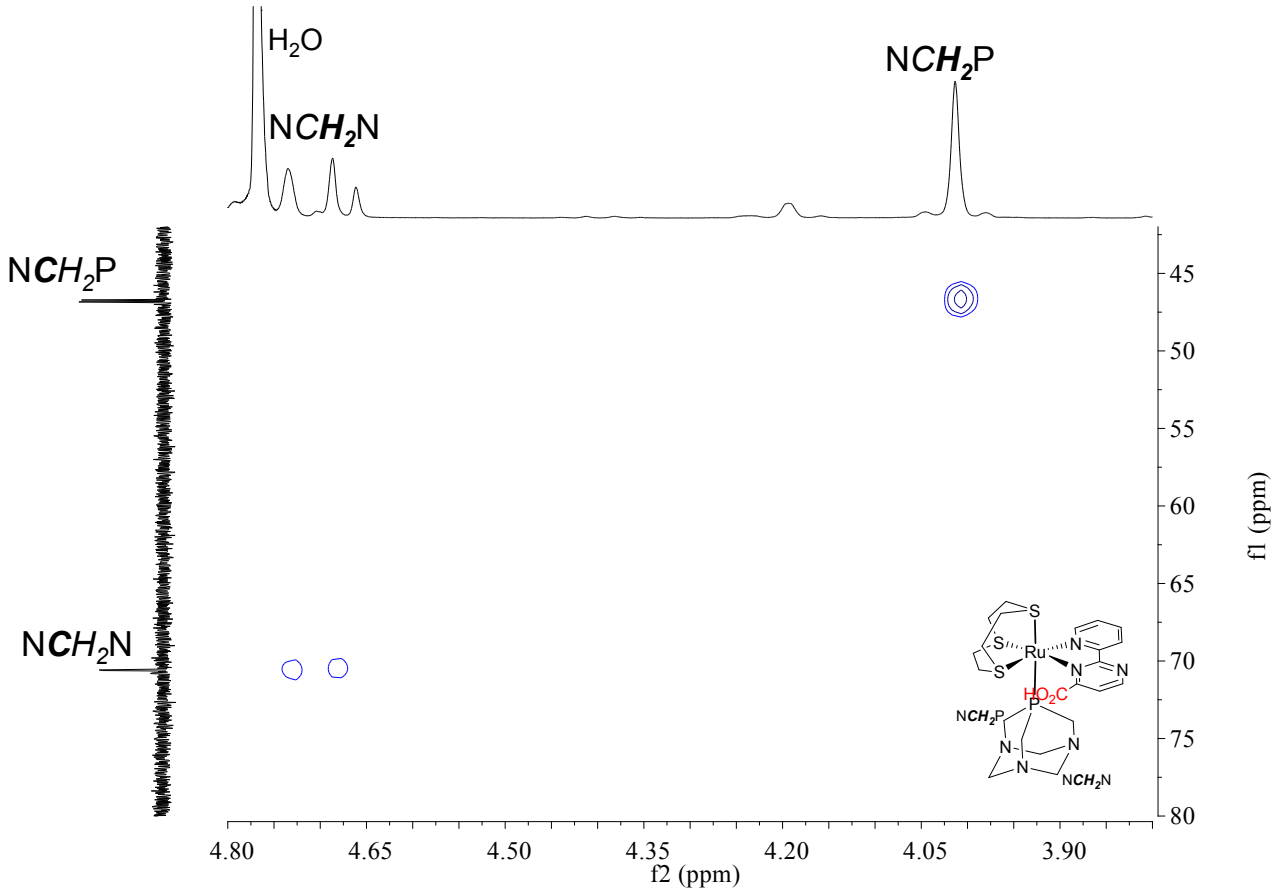

Figure S10. H-C HSQC spectrum (PTA region) of **2*N*^{o}** in D_2O, with labeling scheme.

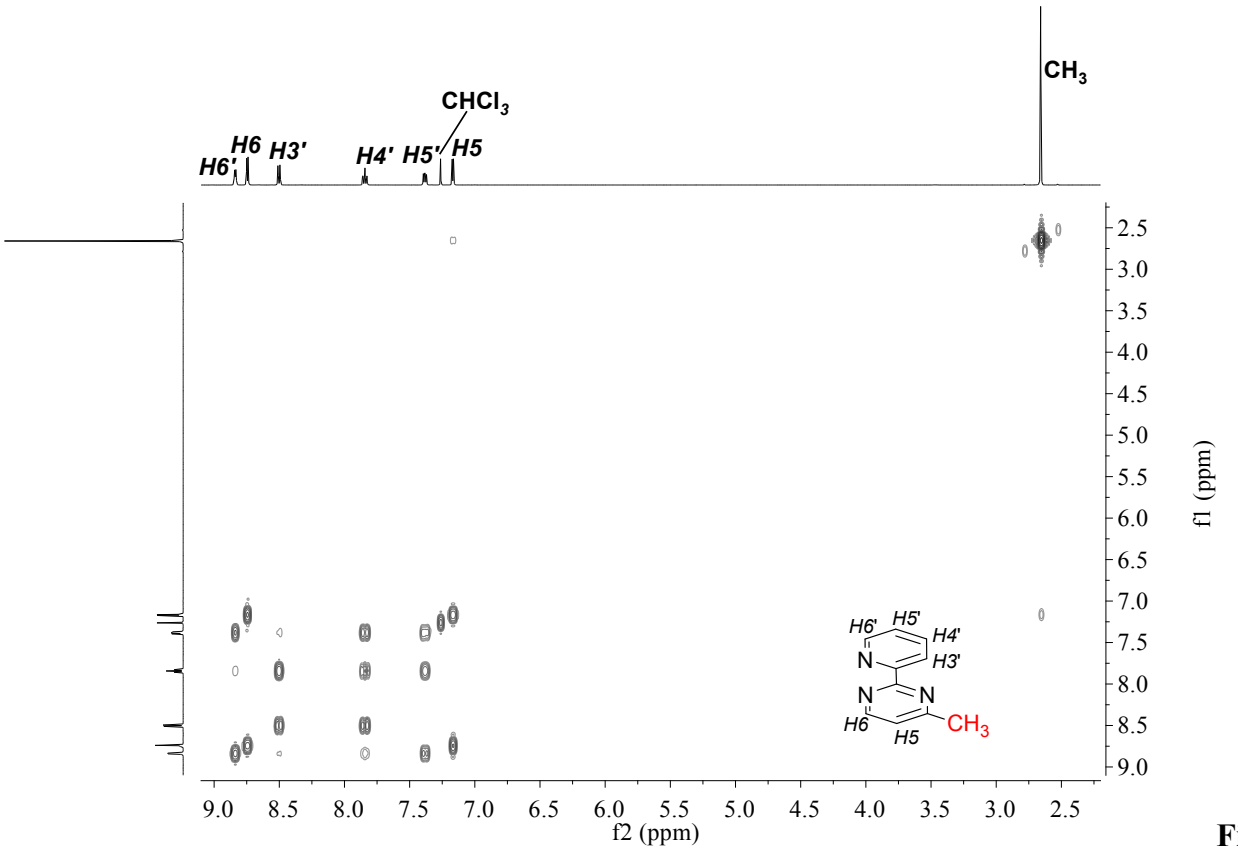

Figure S11. H-H COSY spectrum (downfield region) of **4*N*^{p}** in D_2O, with labeling scheme.

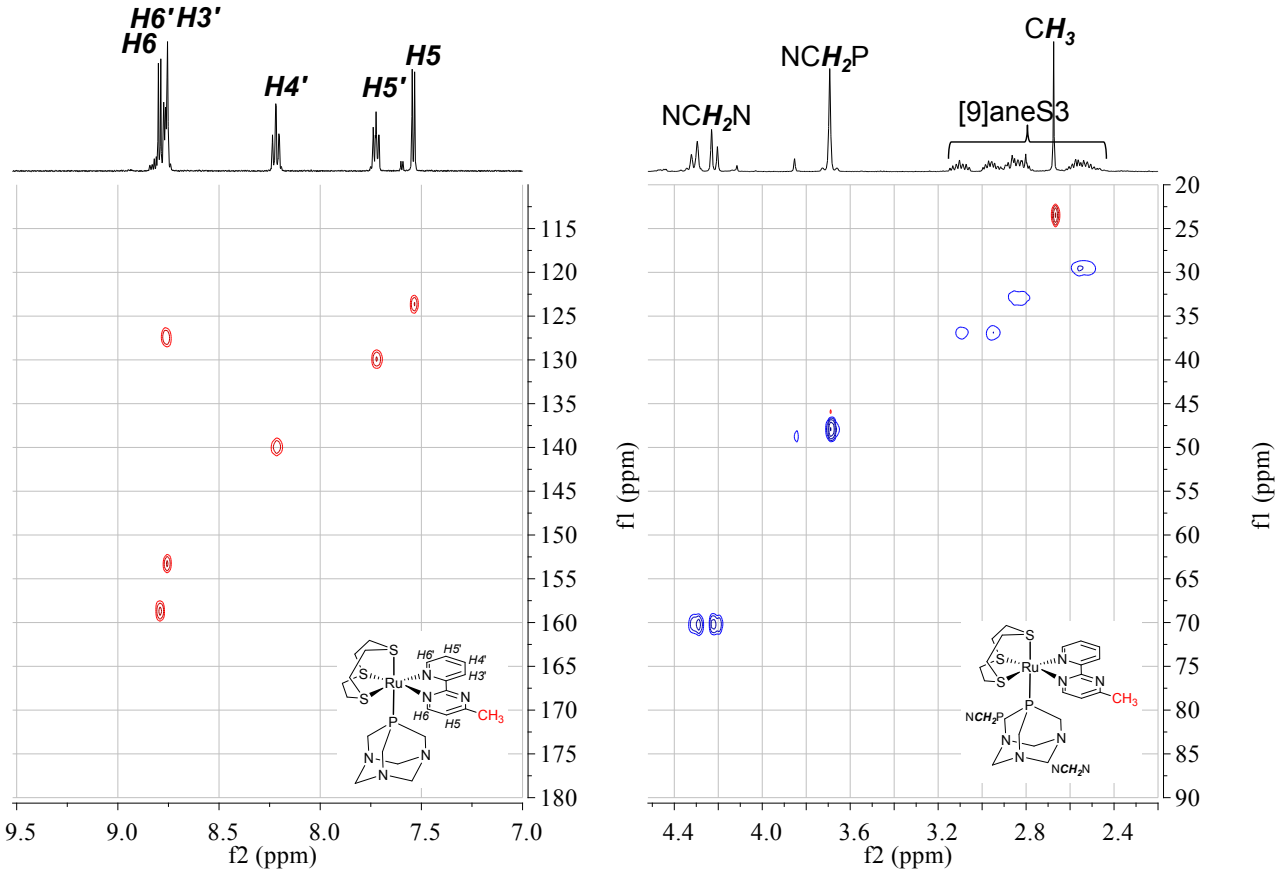

Figure S12. H-C HSQC spectrum (downfield region, left; highfield region, right) of ***4N***^{p} in D_2O, with labeling scheme.

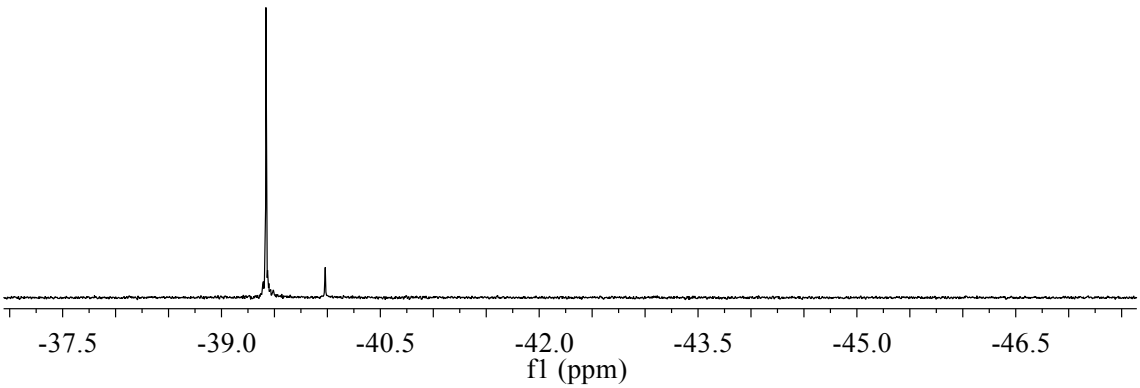

Figure S13. ^{31}P NMR spectrum of crude **4** in D_2O.

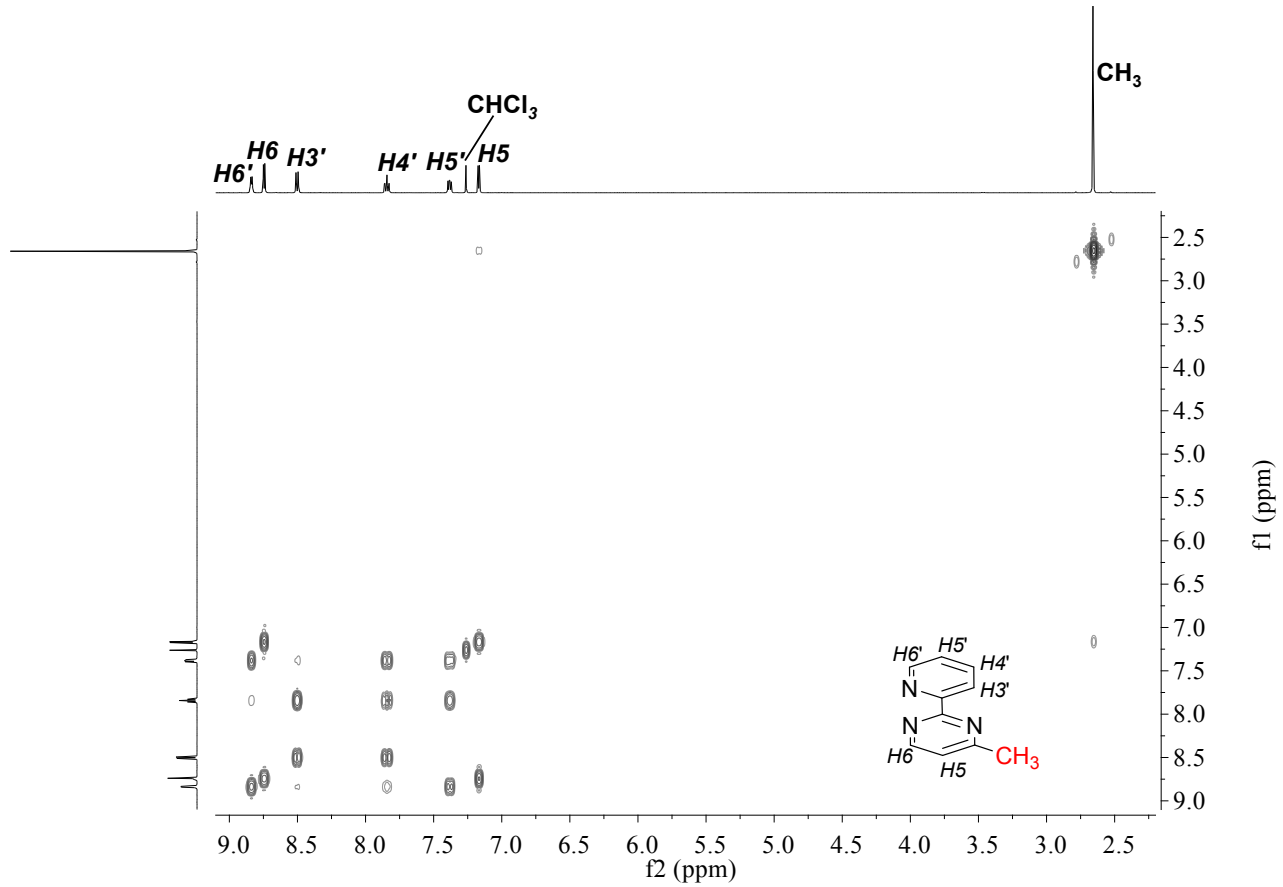

Figure S14. H-H COSY spectrum of **mpp** in $CDCl_3$, with labeling scheme.

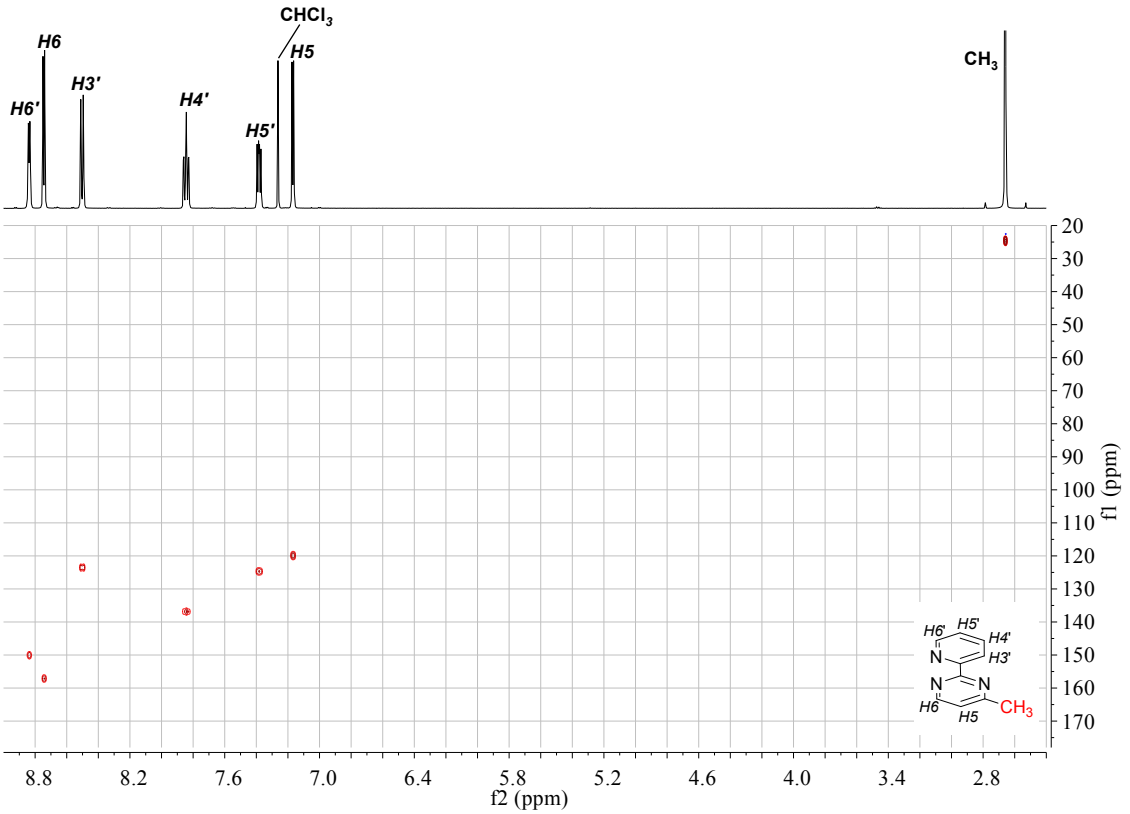

Figure S15. H-C HSQC spectrum of **mpp** in $CDCl_3$, with labeling scheme.

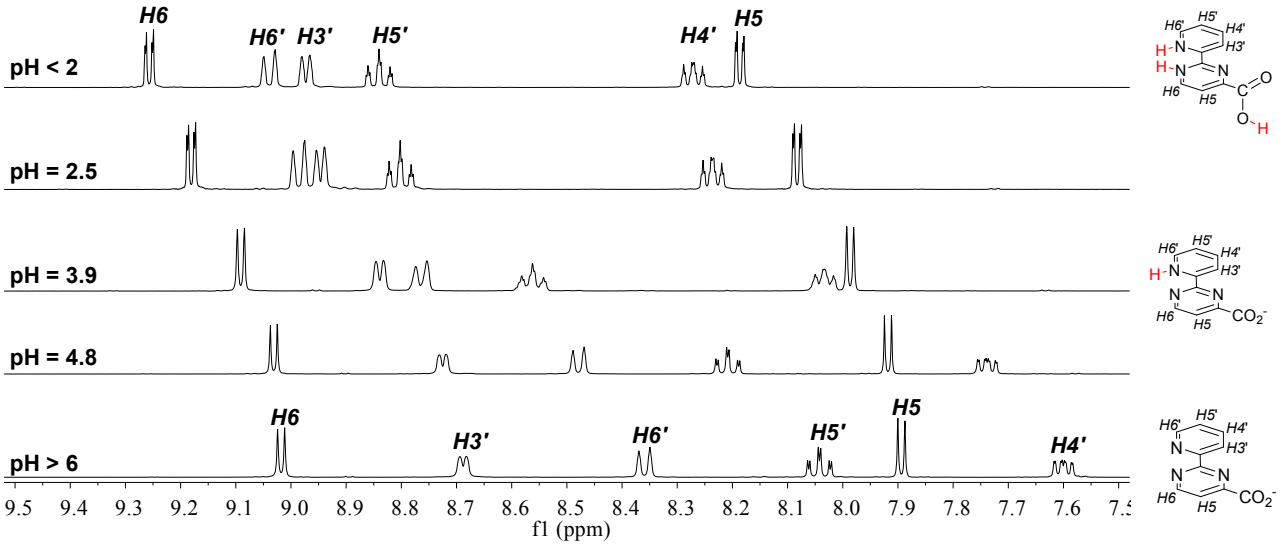

Figure S16. ^{1}H-NMR pH titration of **cppH** in D_2O, with progressive addition of NaOD, and labeling scheme.

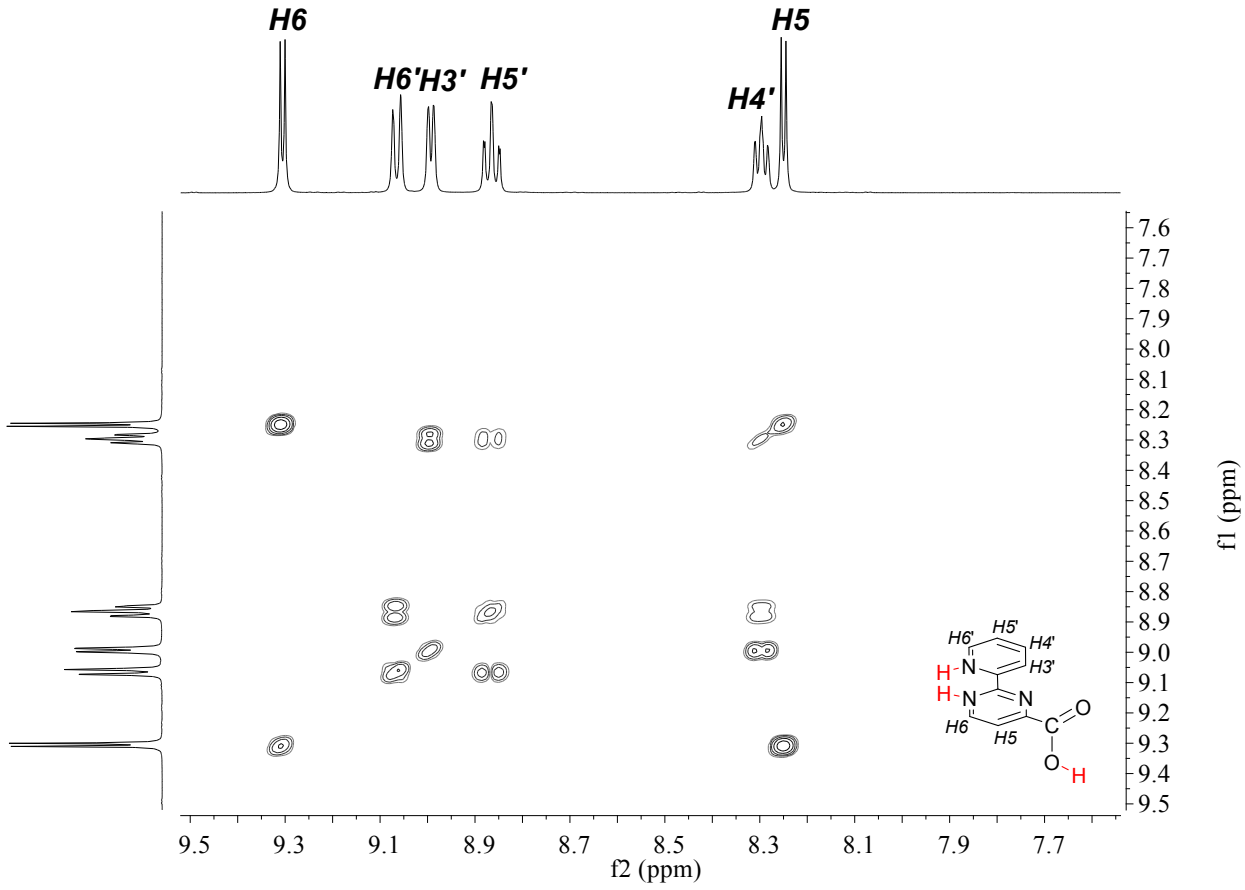

Figure S17. H-H COSY spectrum of **cppH** in D_2O at pH < 2, with labeling scheme.

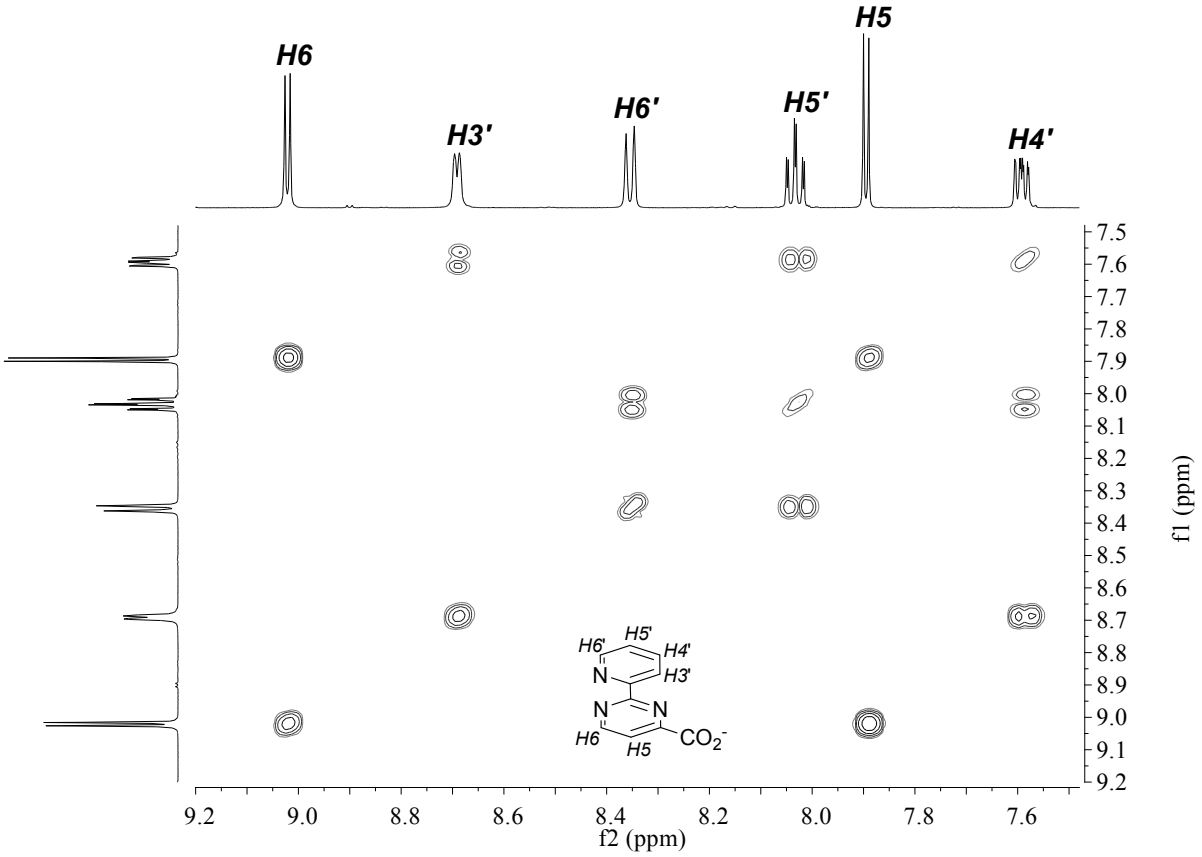

Figure S18. H-H COSY spectrum of **cppH** in D_2O at pH > 6, with labeling scheme.

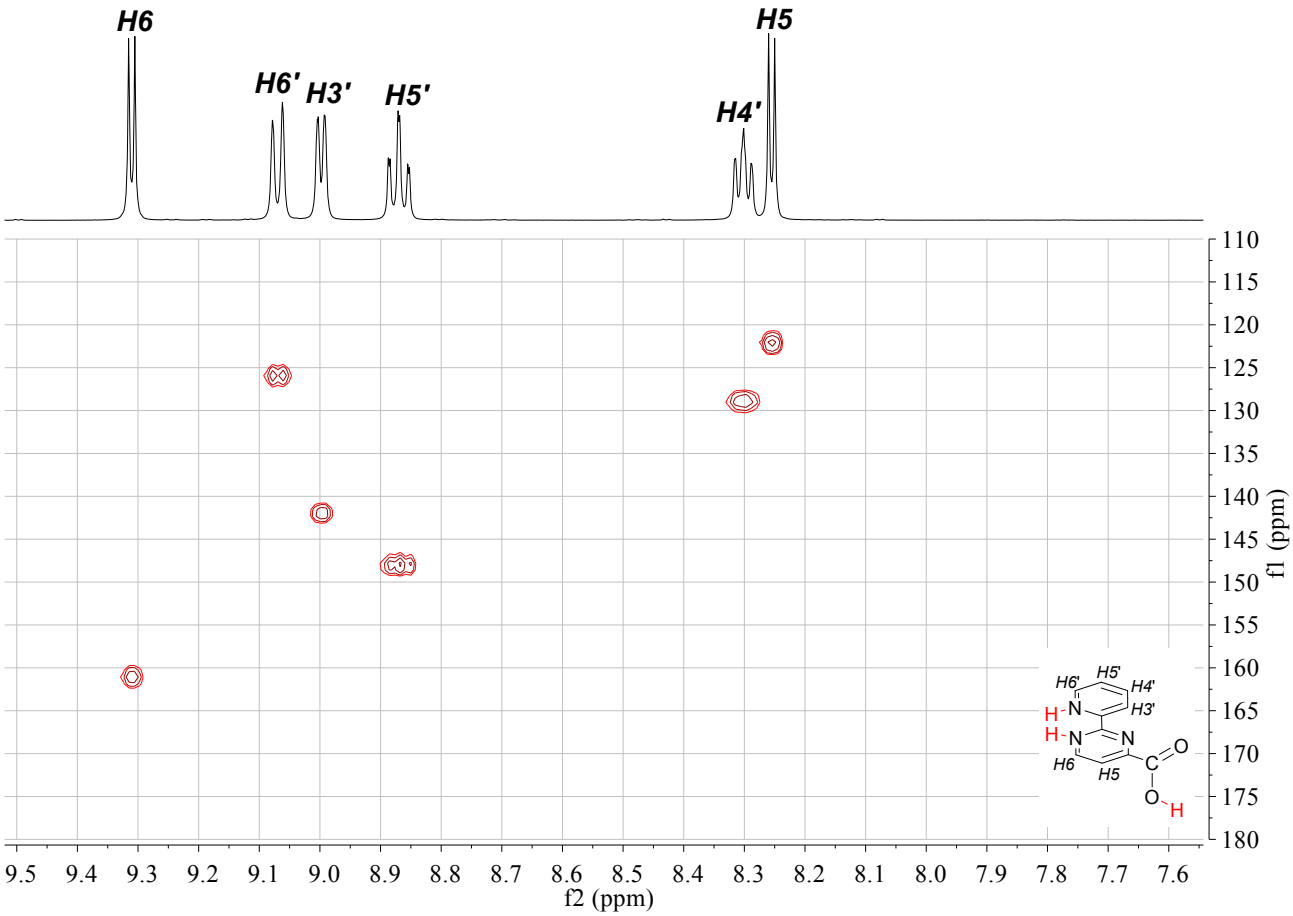

Figure S19. H-C HSQC spectrum of **cppH** in D_2O at pH < 2, with labeling scheme.

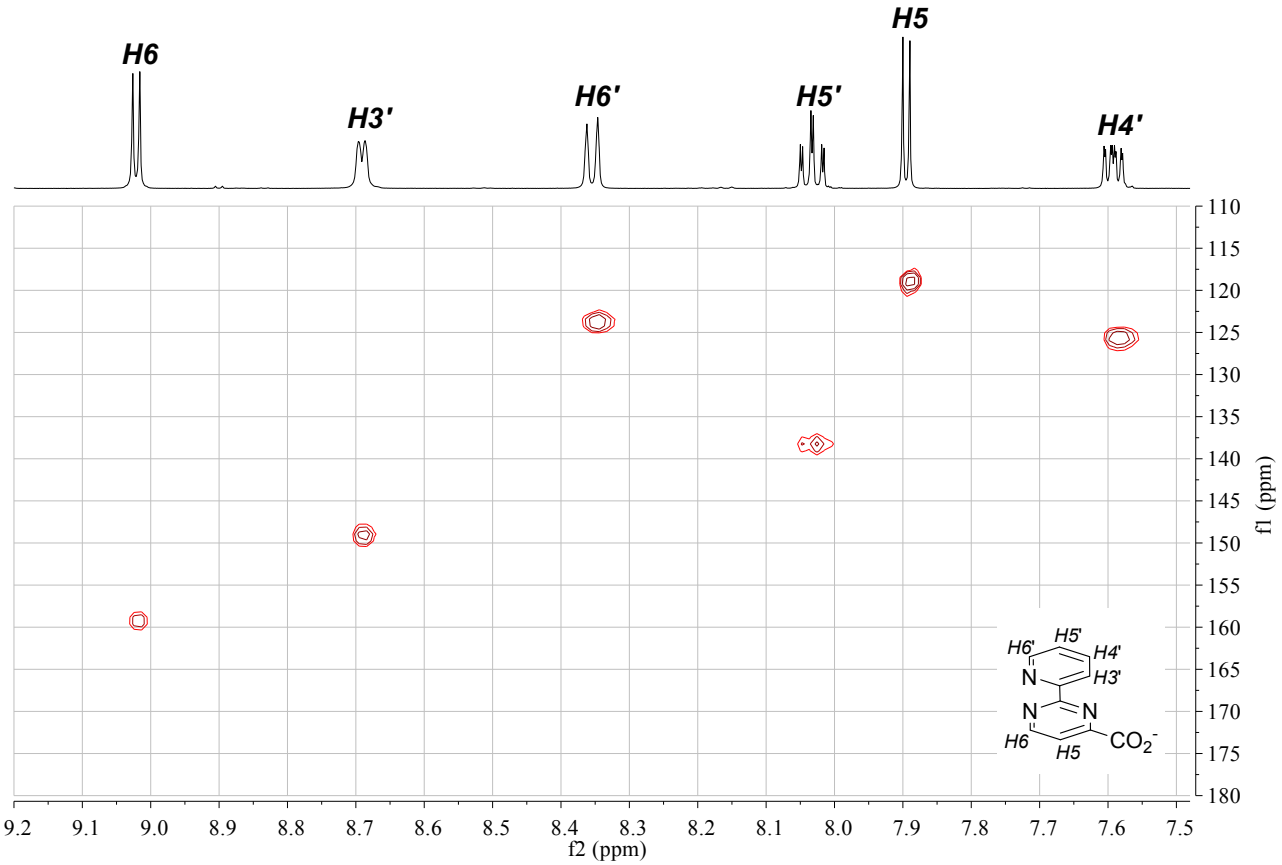

Figure S20. H-C HSQC spectrum of **cppH** in D_2O at pH > 6, with labeling scheme.

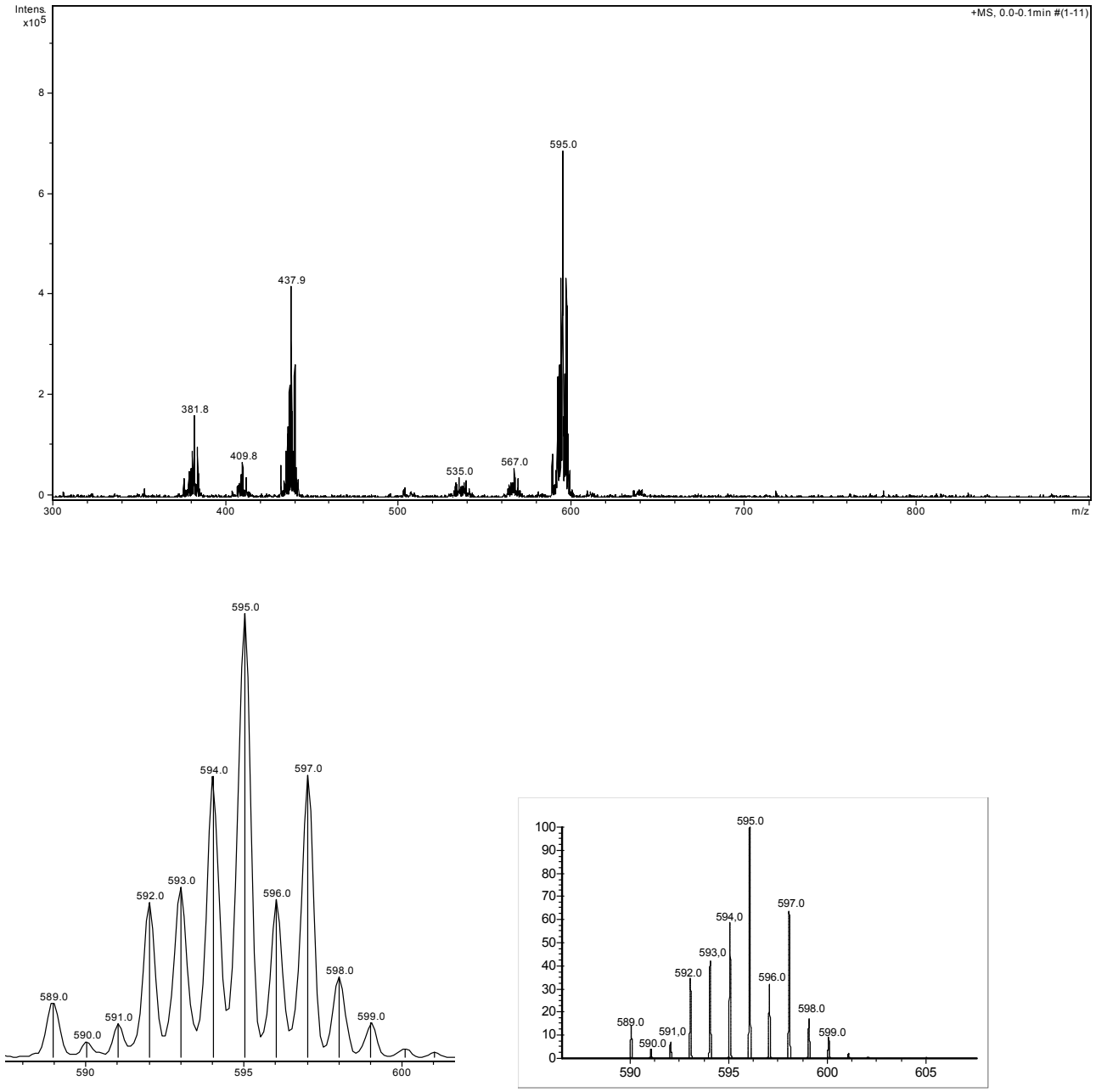

Figure S21. Top: ES mass spectrum (*m*/*z*) (positive mode) of **2*N*^{p}**. Bottom: experimental isotopic distribution of the $(M - H - CO_2)^+$ peak centered at *m*/*z* 595 (left) and simulated pattern (right).

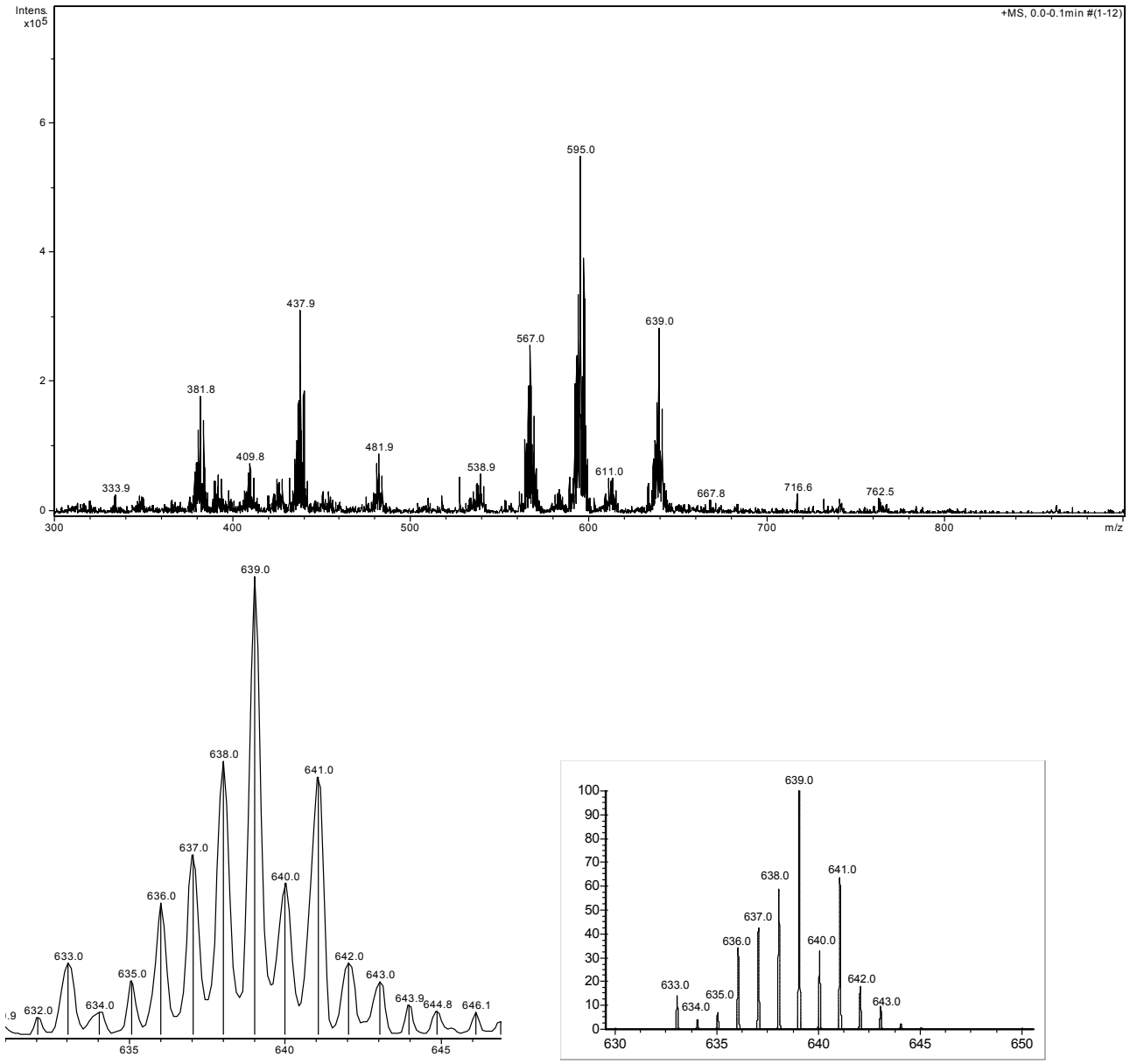

Figure S22. Top: ES mass spectrum (*m*/*z*) (positive mode) of **2*N*^{o}**. Bottom: experimental isotopic distribution of the $(M - H)^+$ peak centered at *m*/*z* 639 (left) and simulated pattern (right).

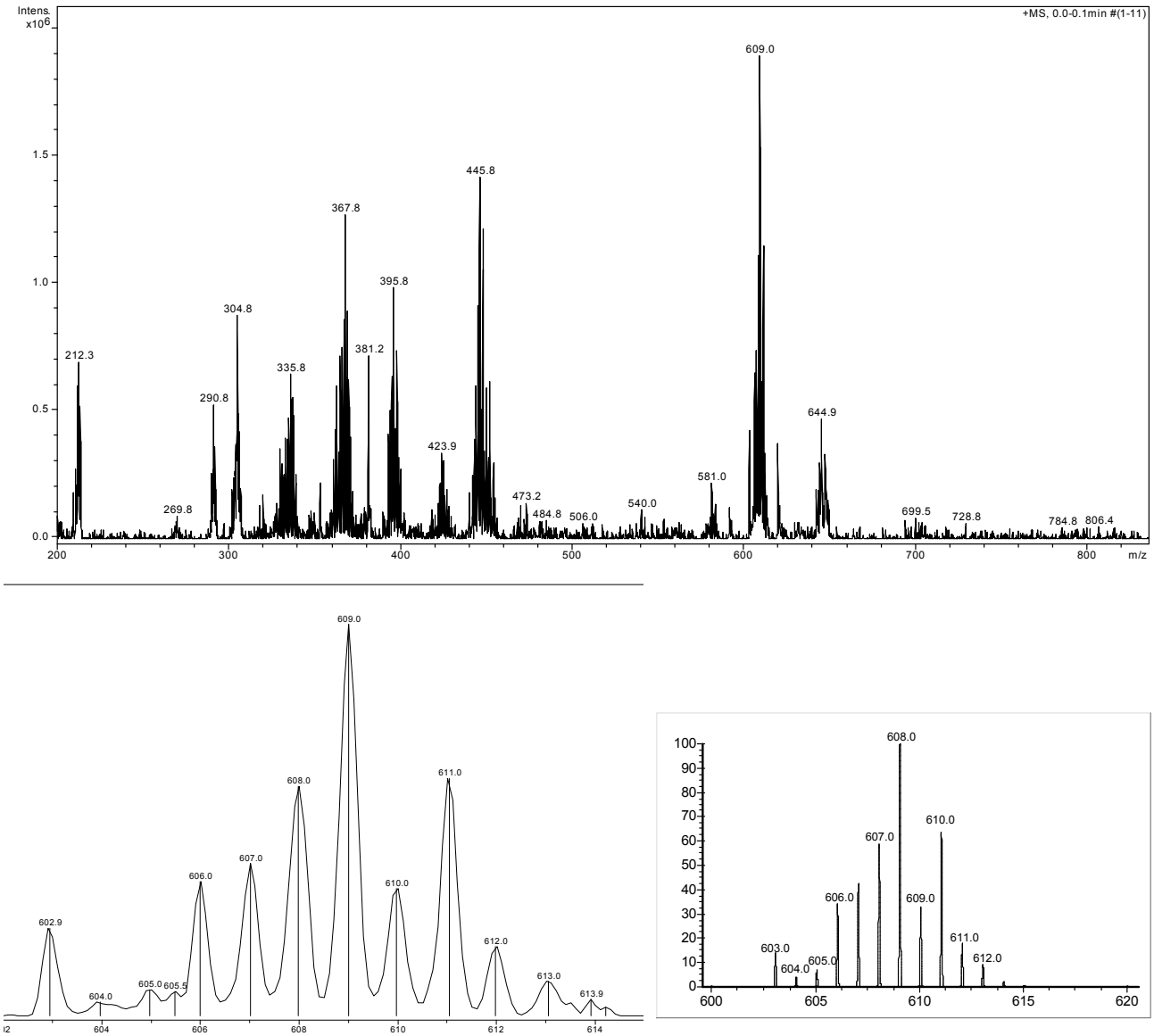

Figure S23. Top: ES mass spectrum (*m*/*z*) (positive mode) of **4*N*^{p}**. Bottom: experimental isotopic distribution of the $(M - H)^+$ peak centered at *m*/*z* 609 (left) and simulated pattern (right).

X-ray diffraction

Data collections were performed at the X-ray diffraction beamline (XRD1) of the Elettra Synchrotron, Trieste (Italy), with a Pilatus 2M image plate detector. Complete datasets were collected at 100 K (nitrogen stream supplied through an Oxford Cryostream 700) with a monochromatic wavelength of 0.700 Å through the rotating crystal method. The crystals of compounds **2*N*^{p}**, **2*N*^{o}**, **3PF$_6$** and **4*N*^{p}** were dipped in N-paratone and mounted on the goniometer head with a nylon loop. The diffraction data were indexed, integrated and scaled using XDS.[1S] Complete datasets for the triclinic crystal forms of compounds **2*N*^{p}** and **4*N*^{p}** were obtained by merging (for each compound) two different data collections done on the same crystal with different orientations. The structures were solved by direct methods using SIR2011,[2S] Fourier analyzed and refined by the full-matrix least-squares based on F^2 implemented in SHELXL-2013.[3S] The Coot program was used for modeling.[4S] Anisotropic thermal motion modeling was then applied to atoms with full occupancy and chlorine atoms with occupancy equal to, or greater than, 50%. Hydrogen atoms were included (except for disordered water molecules) at calculated positions with isotropic $U_{factors} = 1.2\ U_{eq}$. Each stereoisomer crystallized as a racemic mixture in a centrosymmetric space group, *P-1* for **2*N*^{p}** and **4*N*^{p}**, *Pcab* for **2*N*^{o}**, respectively. Whereas the asymmetric units of **2*N*^{p}** and **4*N*^{p}** contain one complex molecule only, that of **2*N*^{o}** contains two identical enantiomers.

Both stereoisomers **2*N*^{p}** and **2*N*^{o}** showed disorder on one chloride counter-ion and on the water molecules that occupy the crystal cavities, forming an extended hydrogen bond network. In the structure of **2*N*^{p}** two full occupancy and one disordered water molecules have been modeled. A region of diffuse disordered electron density has been identified, probably connected to several averaged solvent waters. The contribution of this region to the scattering was estimated as ca. 57 electrons/cell, in a volume of *ca.* 239 Å^3 and it was removed with the SQUEEZE routine of PLATON.[5S] The formula mass and unit-cell characteristics reported for **2*N*^{p}** do not take into account this disordered solvent. In the structure of **2*N*^{o}** three full occupancy water molecules have been modeled and the remaining electron density could be assigned to 16 partially occupied water sites. For **4*N*^{p}**, one chloride shows disorder and three water molecules with full occupancy have been modeled.

Essential crystal and refinement data (Table S1), together with selected bond distances and angles (Tables S2 – S5), are reported below.

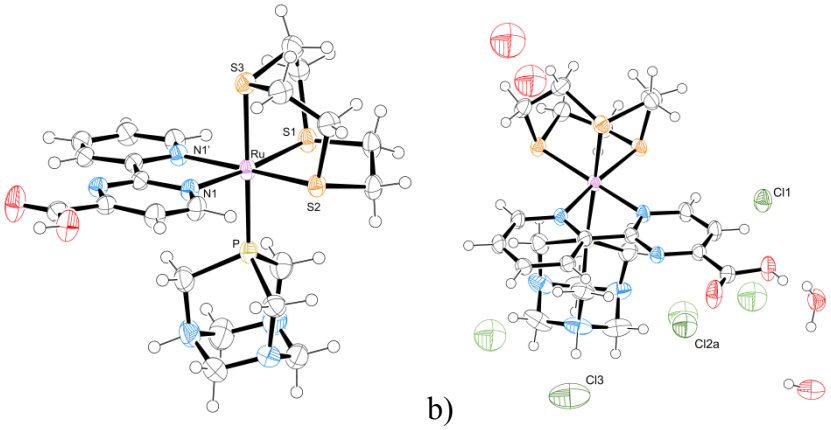

a) b)

Figure S24. X-ray structure (50% probability ellipsoids) of [Ru([9]aneS$_3$)(cppH)(PTA)][Cl$_2$] (***2N^p***) with: a) labeling scheme for Ru coordination sphere; b) full asymmetric unit content. Chlorine anion Cl2 is disordered over four sites: the site with highest occupancy (35%) is labeled Cl2a (for clarity, the other sites are not labeled and are shown with light green ellipsoids). Chlorine atom Cl3 has 50% occupancy and counterbalances the partial protonation of the PTA ligand.

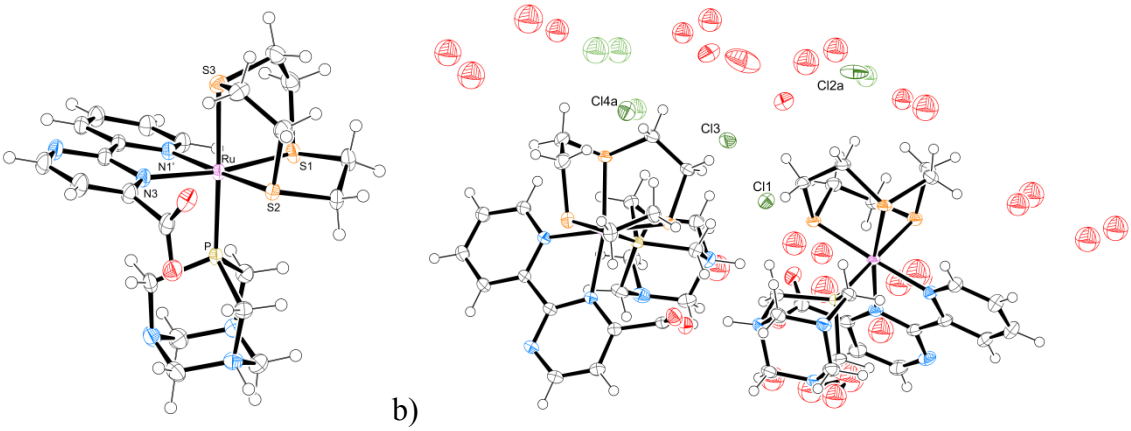

a) b)

Figure S25. X-ray structure (50% probability ellipsoids) of [Ru([9]aneS$_3$)(cpp)(PTAH)][Cl$_2$] (***2N^o***) with: a) labeling scheme for Ru coordination sphere; b) full asymmetric unit content. Chlorine anions Cl2 and Cl4 are disordered: the sites with highest occupancy are labeled Cl2a (85% occupancy) and Cl4a (50% occupancy), respectively. For clarity, the other sites are not labeled and are shown with light green ellipsoids.

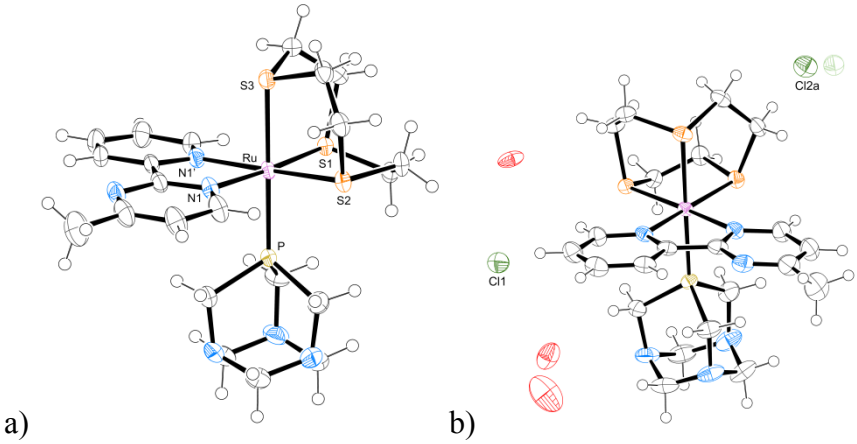

a) b)

Figure S26. X-ray structure (50% probability ellipsoids) of [Ru([9]aneS$_3$)(mpp)(PTA)][Cl$_2$] (***4N^p***) with: a) labeling scheme for Ru coordination sphere; b) full asymmetric unit content. Chlorine anion Cl2 is disordered: the site with highest occupancy (90%) is labeled Cl2a (for clarity, the other site is not labeled and is shown with a light green ellipsoid).

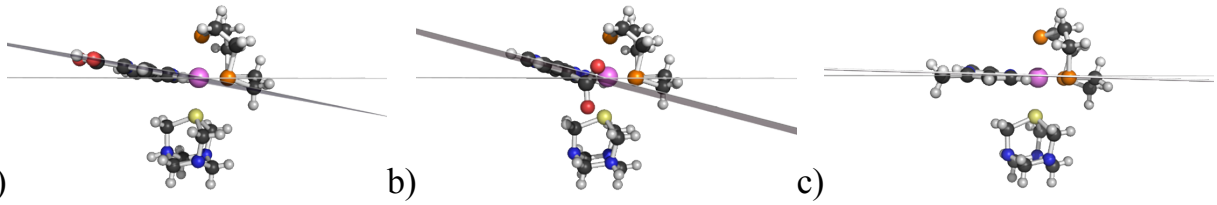

a) b) c)

Figure S27. Ball and stick representation of: a) ***2N^p***, b) ***2N^o***, c) ***4N^p***. The horizontal plane (grey line) is the mean equatorial plane (i.e. the plane containing Ru and the in-plane heteroatoms that bind the metal from cppH/mpp and [9]aneS$_3$). The angle between this plane and the mean cppH/mpp plane (dark grey), obtained by averaging the two heterocycles of the ligand, is ca. 6° in ***2N^p***, ca. 16° in ***2N^o*** and ca. 3° in ***4N^p***.

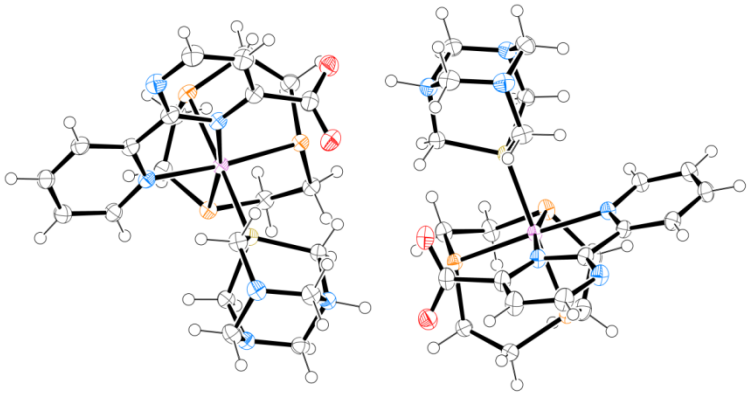

Figure S28. X-ray structure (50% probability ellipsoids) of [Ru([9]aneS$_3$)(cpp)(PTAH)][Cl$_2$] (**2*N*^{o}**), showing the formation, in the crystal lattice, of dimers composed of two molecules with the same chirality. The formation of intermolecular hydrogen bonds between cpp$^-$ and PTAH$^+$ residues keeps the two molecules tightly bonded.

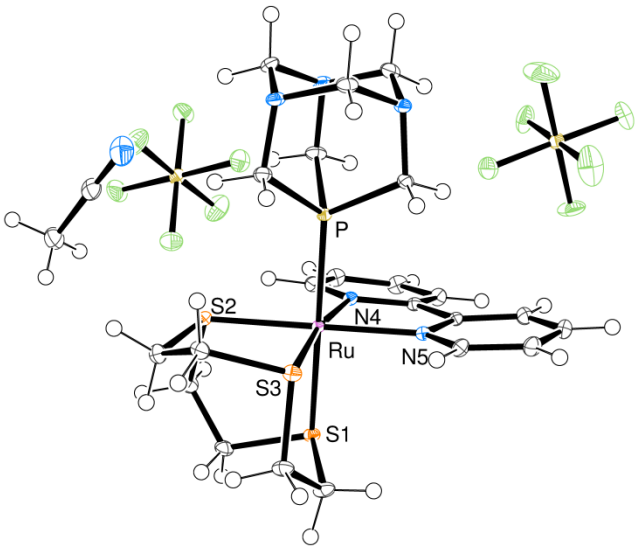

Figure S29. X-ray structure (50% probability ellipsoids) of [Ru([9]aneS$_3$)(bpy)(PTA)][PF$_6$]$_2$·CH$_3$CN (**3PF$_6$**).

Table S1. Crystallographic data and refinement details for compounds **2*N*^{p}** and **2*N*^{o}**.

	[Ru([9]aneS$_3$)(cppH)(PTAH$_{0.5}$)][Cl$_{2.5}$]·2.75H$_2$O (**2*N*^{p}**)	[Ru([9]aneS$_3$)(cpp)(PTAH)][Cl$_2$]·6.25H$_2$O (**2*N*^{o}**)
Moiety Formula	C$_{22}$H$_{31.5}$N$_6$O$_2$PRuS$_3$, 2.5(Cl), 2.75(H$_2$O)	2(C$_{22}$H$_{31}$N$_6$O$_2$PRuS$_3$, 4(Cl), 12.5(H$_2$O)
Empirical Formula	C$_{22}$H$_{35.5}$N$_6$O$_{4.75}$PRuS$_3$Cl$_{2.5}$	C$_{44}$H$_{62}$N$_{12}$O$_{16.5}$P$_2$Ru$_2$S$_6$Cl$_4$
Formula weight (Da)	776.91	1621.29
Temperature (K)	100(2)	100(2)
Wavelength (Å)	0.700	0.700
Crystal system	Triclinic	Orthorombic
Space Group	*P-1*	*Pcab*
a (Å)	10.8640(5)	20.543(6)
b (Å)	12.5130(3)	24.132(4)
c (Å)	15.2790(8)	28.016(3)
α (°)	112.547(5)	90
β (°)	105.610(4)	90
γ (°)	96.533(4)	90
V (Å^3)	1791.7(2)	13889(5)
Z	2	8
ρ (g·cm^{-3})	1.440	1.551
F(000)	794.0	6592.0
μ (mm^{-1})	0.767	0.766
θ min,max (°)	1.5, 25.9	2.1, 29.1
Resolution (Å)	0.80	0.72
Total refl. collctd	67678	290038
Independent refl.	7033	19288
Obs. Refl. [Fo>4σ(Fo)]	6934	17393
I/σ(I) (all data)	66.1	30.0
I/σ(I) (max resltn)	63.4	27.5
Completeness (all data)	0.96	1.00
Completeness (max resltn)	0.96	1.00
Rmerge (all data)	0.020	0.036
Rmerge (max resltn,)	0.020	0.042
Multiplicity (all data)	6.4	6.4
Multiplicity (max resltn)	6.5	6.4
Data/restraint/parameters	7033/230/390	19288/473/815
Goof	1.239	1.028
R[I>2.0σ(I)], wR2 [I>2.0σ(I)]	0.0467, 0.1253	0.0373, 0.0970
R (all data), wR2 (all data)	0.0469, 0.1255	0.0413, 0.1001

Table S1 contd. Crystallographic data and refinement details for compounds **3PF$_6$** and **4*N*^{p}**.

	[Ru([9]aneS$_3$)(bpy)(PTA)][PF$_6$]$_2$·CH$_3$CN (**3PF$_6$**)	[Ru([9]aneS$_3$)(mpp)(PTA)][Cl$_2$]·3H$_2$O (**4*N*^{p}**)
Moiety Formula	$C_{22}H_{32}N_5PRuS_3$, 2(PF_6), C_2H_3N	$C_{22}H_{33}N_6PRuS_3$, 2(Cl), 3(H_2O)
Formula	$C_{24}H_{35}F_{12}N_6P_3RuS_3$	$C_{22}H_{39}N_6O_3PRuS_3Cl_2$
Formula weight (Da)	925.74	734.71
Temperature (K)	100(2)	100(2)
Wavelength (Å)	0.700	0.700
Crystal system	Monoclinic	Triclinic
Space Group	*C 2/c*	*P-1*
a (Å)	37.772	10.877(6)
b (Å)	11.250	11.842(2)
c (Å)	16.318	12.902(3)
α (°)	90	102.179(8)
β (°)	108.02	111.389(3)
γ (°)	90	91.558(3)
V (Å^3)	6593.8	1502.6(9)
Z	8	2
ρ (g·cm^{-3})	1.865	1.624
F(000)	3728	756.0
μ (mm^{-1})	0.861	0.868
θ min,max (°)	1.117, 29.978	1.7, 29.1
Resolution (Å)	0.70	0.72
Total refl. collctd	64617	51969
Independent refl.	10063	8163
Obs. Refl. [Fo>4σ(Fo)]	9511	7195
I/σ(I) (all data)	40.4	11.40
I/σ(I) (max resltn)	37.8	7.86
Completeness (all data)	0.96	0.94
Completeness (max resltn)	0.92	0.92
Rmerge (all data)	0.039	0.061
Rmerge (max resltn)	0.024	0.090
Multiplicity (all data)	6.4	3.0
Multiplicity (max resltn)	6.4	2.9
Data/restraint/parameters	9523/0/443	8163/0/367
Goof	1.205	1.049
R[I>2.0σ(I)], wR2 [I>2.0σ(I)]	0.0327, 0.0824	0.0464, 0.1242
R (all data), wR2 (all data)	0.0327, 0.0824	0.0521, 0.1203

Table S2. Selected coordination distances (Å) and angles (°) for [Ru([9]aneS_3)(cppH)(PTA)][Cl_2] (**2*N*^{p}**).

Bond distances (Å)			
Ru–S(1)	2.3237 (8)	Ru–P	2.2914 (8)
Ru–S(2)	2.3144 (7)	Ru–N(1)	2.0914 (26)
Ru–S(3)	2.3743 (8)	Ru–N(1')	2.1096 (24)
Bond angles (°)			
S(1)–Ru–S(2)	87.30 (3)	S(2)–Ru–N(1')	173.21 (7)
S(1)–Ru–S(3)	87.22 (3)	S(3)–Ru–P	178.90 (3)
S(2)–Ru–S(3)	87.82 (3)	S(3)–Ru–N(1)	88.99 (7)
S(1)–Ru–P	92.90 (3)	S(3)–Ru–N(1')	90.16 (7)
S(1)–Ru–N(1)	175.02 (7)	P–Ru–N(1)	91.53 (7)
S(1)–Ru–N(1')	99.08 (7)	P–Ru–N(1')	89.01 (7)
S(2)–Ru–P	93.09 (3)	N(1)–Ru–N(1')	77.69 (10)
S(2)–Ru–N(1)	95.78 (7)		

Table S3. Selected coordination distances (Å) and angles (°) for [Ru([9]aneS_3)(cpp)(PTAH)][Cl_2] (**2*N^o^***); each column refers to one distinct crystallographically independent molecule.

Molecule 1		*Molecule 2*	
Bond distances (Å)			
Ru–S1(1)	2.3103 (5)	Ru–S1(1)	2.3103 (5)
Ru–S1(2)	2.3379 (5)	Ru–S1(2)	2.3360 (5)
Ru–S1(3)	2.3621 (5)	Ru–S1(3)	2.3800 (6)
Ru–P1	2.2934 (5)	Ru–P1	2.2980 (5)
Ru–N1(3)	2.1449 (17)	Ru–N1(3)	2.1461 (17)
Ru–N1(1')	2.0992 (18)	Ru–N1(1')	2.1010 (17)
Bond angles (°)			
S(1)–Ru–S(2)	87.08 (2)	S(1)–Ru–S(2)	86.67 (2)
S(1)–Ru–S(3)	87.71 (2)	S(1)–Ru–S(3)	87.47 (2)
S(2)–Ru–S(3)	87.46 (2)	S(2)–Ru–S(3)	87.93 (2)
S(1)–Ru–P	91.51 (2)	S(1)–Ru–P	93.36 (2)
S(1)–Ru–N(3)	169.85 (5)	S(1)–Ru–N(3)	169.68 (5)
S(1)–Ru–N(1')	94.21 (2)	S(1)–Ru–N(1')	94.19 (5)
S(2)–Ru–P	94.12 (2)	S(2)–Ru–P	93.88 (2)
S(2)–Ru–N(3)	100.87 (5)	S(2)–Ru–N(3)	101.44 (5)
S(2)–Ru–N(1')	174.63 (5)	S(2)–Ru–N(1')	177.11 (5)
S(3)–Ru–P	178.20 (2)	S(3)–Ru–P	178.05 (2)
S(3)–Ru–N(3)	86.36 (5)	S(3)–Ru–N(3)	86.47 (5)
S(3)–Ru–N(1')	87.38 (5)	S(3)–Ru–N(1')	89.35 (5)
P–Ru–N(3)	94.18 (5)	P–Ru–N(3)	92.45 (5)
P–Ru–N(1')	91.06 (5)	P–Ru–N(1')	88.83 (5)
N(3)–Ru–N(1')	77.31 (7)	N(3)–Ru–N(1')	77.41 (7)

Table S4. Selected coordination distances (Å) and angles (°) for [Ru([9]aneS$_3$)(bpy)(PTA)][PF$_6$]$_2$ (**3PF$_6$**).

Bond distances (Å)			
Ru–S(1)	2.3647(3)	Ru–P	2.3157(4)
Ru–S(2)	2.3145(3)	Ru–N(4)	2.0959(11)
Ru–S(3)	2.3147(3)	Ru–N(5)	2.0970(11)
Bond angles (°)			
S(1)–Ru–S(2)	87.263(12)	S(2)–Ru–N(5)	176.69(3)
S(1)–Ru–S(3)	87.926(12)	S(3)–Ru–P	95.473(13)
S(2)–Ru–S(3)	87.489(11)	S(3)–Ru–N(4)	171.46(3)
S(1)–Ru–P	176.470(12)	S(3)–Ru–N(5)	95.64(3)
S(1)–Ru–N(4)	86.56(3)	P–Ru–N(4)	90.17(3)
S(1)–Ru–N(5)	91.77(3)	P–Ru–N(5)	88.85(3)
S(2)–Ru–P	91.926(12)	N(4)–Ru–N(5)	78.03(4)
S(2)–Ru–N(4)	98.75(3)		

Table S5. Selected coordination distances (Å) and angles (°) for [Ru([9]aneS$_3$)(mpp)(PTA)][Cl$_2$] (**4*N*^{p}**).

Bond distances (Å)			
Ru–S(1)	2.3110 (8)	Ru–P	2.2967 (8)
Ru–S(2)	2.3174 (11)	Ru–N(1)	2.0965 (24)
Ru–S(3)	2.3787 (8)	Ru–N(1')	2.0985 (24)
Bond angles (°)			
S(1)–Ru–S(2)	87.36 (4)	S(2)–Ru–N(1')	174.76 (7)
S(1)–Ru–S(3)	87.71 (3)	S(3)–Ru–P	179.32 (3)
S(2)–Ru–S(3)	88.09 (3)	S(3)–Ru–N(1)	90.94 (7)
S(1)–Ru–P	92.95 (3)	S(3)–Ru–N(1')	89.21 (7)
S(1)–Ru–N(1)	174.65 (7)	P–Ru–N(1)	88.41 (7)
S(1)–Ru–N(1')	97.03 (8)	P–Ru–N(1')	90.84 (7)
S(2)–Ru–P	91.80 (3)	N(1)–Ru–N(1')	77.77 (10)
S(2)–Ru–N(1)	97.77 (8)		

References

[S1] W. Kabsch, *Acta Cryst. D* **2010**, *66*, 125–132.

[S2] M. C. Burla, R. Caliandro, M. Camalli, B. Carrozzini, G. L. Cascarano, C. Giacovazzo, M. Mallamo, A. Mazzone, G. Polidori, R. Spagna, *J. Appl. Cryst.* **2012**, *45*, 357–361.

[S3] G. M. Sheldrick, T. R. Schneider, *Methods Enzymol.* **1997**, *277*, 319–343.

[S4] P. Emsley, K. Cowtan, *Acta Cryst. D* **2004**, *60*, 2126–2132.

[S5] A. L. Spek, *Acta Cryst. D* **2009**, *65*, 148–155.